

MOL #34371

## Title page

### Complete title of the manuscript:

Mechanism of thiazolidinedione-dependent cell death in Jurkat T cells<sup>1</sup>

### Authors:

Mathias Soller, Stefan Dröse, Ulrich Brandt, Bernhard Brüne, Andreas von Knethen

Department of Biochemistry I - Pathobiochemistry (M.S., B.B., A.v.K.) and Molecular Bioenergetics (S.D., U.B.), Johann Wolfgang Goethe-University Frankfurt, Faculty of Medicine, 60590 Frankfurt am Main, Germany

### Primary laboratory of origin:

Department of Biochemistry I - Pathobiochemistry, Johann Wolfgang Goethe-University Frankfurt, Faculty of Medicine, 60590 Frankfurt am Main, Germany

MOL #34371

## Running title page

### Running title:

TZD-induced cell death by PPAR $\gamma$ -independent mechanisms.

### Address of correspondence:

Andreas von Knethen, Department of Biochemistry I - Pathobiochemistry, Johann Wolfgang Goethe-University, Faculty of Medicine, Theodor-Stern-Kai 7, 60590 Frankfurt/Main, Germany, Phone: +49-69-6301 6989; Fax: +49-69-6301 4203; E-Mail: v\_knethen@zbc.kgu.de

**Number of pages: 32**

**Number of figures: 11**

**Number of references: 39**

**Number of words in the abstract: 246**

**Number of words in the introduction: 535**

**Number of words in the discussion: 1453**

### List of abbreviations:

2-DG, 2-deoxy-D-glucose; CIG, ciglitazone; Cyt *c*, cytochrome *c*; DAPI, 4',6-diamidino-2-phenylindol; DBQ, n-decylubiquinone; DCIP, dichlorophenolindophenol; DiOC6(3), 3,3'-dihexyloxacarbocyanide iodide; H<sub>2</sub>DCF-DA, 2',7'-dichlorodihydrofluorescein diacetate; MnTBAP, manganese (III) tetrakis (4-benzoic acid) porphyrin; NAC, N-acetyl-cysteine; PI, propidiumiodide; PPAR $\gamma$ , peroxisome proliferator-activated receptor gamma; ROSI, rosiglitazone; Rot, rotenone; SMP, submitochondrial particle; STS, staurosporine; TRO, troglitazone; TTFA, 2-thenoyltrifluoroacetone; TZD, thiazolidinedione

MOL #34371

## Abstract

### ABSTRACT

Thiazolidinediones are synthetic agonists for the transcriptionfactor peroxisome proliferator-activated receptor  $\gamma$  (PPAR $\gamma$ ) and are therapeutically used as insulin sensitizers. Besides therapeutical benefits, potential side effects like induction of cell death by thiazolidinediones deserve consideration. Although PPAR $\gamma$ -dependent and -independent cell death in response to thiazolidinediones has been described, we provide evidence supporting a new mechanism to account for thiazolidinedione-initiated but PPAR $\gamma$ -independent cell demise. In Jurkat T cells ciglitazone and troglitazone provoked rapid and dose-dependent cell death, while rosiglitazone did not alter cell viability. We found induction of apoptosis by troglitazone whereas ciglitazone caused necrosis. Since preincubation with the ROS scavengers manganese (III) tetrakis (4-benzoic acid) porphyrin and vitamin c significantly inhibited ciglitazone- and partially troglitazone-mediated cell death we suggest that ROS contribute to cytotoxicity. Assuming that ROS originate from mitochondria, studies in submitochondrial particles demonstrated that all thiazolidinediones inhibited complex I of the mitochondrial respiratory chain. However, only ciglitazone and troglitazone lowered complex II activity as well. Pharmacological inhibition of complexes I and II documented that complex II inhibition in Jurkat cells caused massive apoptotic cell death whereas inhibition of complex I provoked only marginally apoptosis after 4 h treatment. Therefore, inhibition of complex II by ciglitazone and troglitazone is the main trigger of cell death. ATP depletion by ciglitazone, in contrast to troglitazone, is responsible for induction of necrosis. Our results demonstrate that despite their similar molecular structure thiazolidinediones differently affect cell death, which might help to explain some adverse effects occurring during thiazolidinedione-based therapies.

MOL #34371

## Introduction

The transcription factor peroxisome proliferator-activated receptor gamma (PPAR $\gamma$ ) is a member of the nuclear hormone receptor superfamily. Three isoforms PPAR $\alpha$ , PPAR $\beta/\delta$  and PPAR $\gamma$  have been identified so far. Among these, PPAR $\gamma$  is best characterized due to its therapeutic potential for treatment of diabetes type 2. However, PPAR $\gamma$  is also known for its involvement in several other human pathological settings including atherosclerosis, cancer and inflammation (Kersten et al., 2000). DNA binding by PPAR $\gamma$  as a transcription factor requires heterodimerization with the 9-cis-retinoic acid receptor (RXR) and binding of an agonist. Natural agonists of PPAR $\gamma$  originate from the metabolism of arachidonic acid, including leukotrienes, hydroxyeicosatetraenoic acids and prostaglandins (Daynes and Jones, 2002). Thiazolidinediones (TZDs) such as ciglitazone, troglitazone and rosiglitazone represent a group of synthetic PPAR $\gamma$  agonists. Most synthetic agonists belong to the class of above mentioned TZDs but also non-TZD synthetic agonists have been described (Rybczynski et al., 2003). Activated PPAR $\gamma$ , especially in T cells, is involved in the regulation of immune-responses and cell survival signaling (Harris and Phipps, 2000; Harris and Phipps, 2001; Harris and Phipps, 2002; Soller et al., 2006; Tautenhahn et al., 2003). This finding is important in type 2 diabetic patients, medicated by TZDs as known insulin-sensitizers. Therefore, activation of PPAR $\gamma$  in these patients might provoke an inhibited immune-response by the induction of cell death.

However, actions of TZDs are currently discussed due to the increasing number of publications describing their effects by activating pathways independently from PPAR $\gamma$  signaling. The argumentation that TZDs can exert receptor-independent effects is based on observations that concentrations needed to observe TZD actions were much higher than their EC<sub>50</sub> values, PPAR $\gamma$  antagonists failed to inhibit TZD-evoked responses, effects occurred rapidly and often without



MOL #34371

PPAR $\gamma$  expression (Feinstein et al., 2005). Therefore, we focused our interest in the present study on PPAR $\gamma$ -independent effects of the TZDs ciglitazone, troglitazone and rosiglitazone in Jurkat T cells. Among these mentioned TZDs rosiglitazone is currently used as an anti-diabetic drug, whereas the therapeutic use of troglitazone was stopped due to its liver intoxication (Tolman, 2000).

Recent studies dealing with PPAR $\gamma$ -independent effects of TZDs point at mitochondria as primary targets. In this respect a rapid decrease in mitochondrial membrane potential ( $\Delta\Psi_M$ ) seems to be one major event, especially following troglitazone and ciglitazone treatment. Troglitazone quickly induced mitochondrial dysfunction, increased permeability, calcium influx and nuclear condensation, as well as caspase-3 activation in HepG2 hepatocarcinoma cells (Bova et al., 2005; Haskins et al., 2001). Rapid effects were observed in response to ciglitazone, which also induced break-down of  $\Delta\Psi_M$ , increased ROS production in astrocytes and enhanced lactate production in leukaemia (HL-60) cells (Perez-Ortiz et al., 2004; Scatena et al., 2004). These data suggest that TZDs affect mitochondrial respiration causing changes in the glycolytic metabolism. Indeed, it has been shown that complex I is inhibited by TZDs (Brunmair et al., 2004; Scatena et al., 2004), supporting the hypothesis that several effects attributed to TZDs are due to their impact on mitochondria.

Taking into consideration that TZDs are discussed as therapeutics for the treatment of cancer, various inflammatory and neurodegenerative diseases (Pershad Singh, 2004), beside their current use for the treatment of diabetes type 2, a better understanding of TZD signaling in various tissues is essential for future drug design.

MOL #34371

## Materials and Methods

### MATERIALS AND METHODS

*Materials* - Ciglitazone, troglitazone, rosiglitazone, staurosporine and manganese (III) tetrakis (4-benzoic acid) porphyrin (MnTBAP) were obtained from Alexis (Grünberg, Germany). H<sub>2</sub>DCF-DA was obtained from Molecular Probes (Molecular Probes, Leiden, The Netherlands). All other chemicals were purchased from Sigma (Taufkirchen, Germany) or Carl Roth GmbH & Co. (Karlsruhe, Germany) in analytical quality.

*Cell culture* - We cultivated Jurkat cells in 24well plates (BD Falcon Biosciences, Heidelberg, Germany) using RPMI 1640 medium (Biochrom, Berlin, Germany) supplemented with 100 U/ml penicillin (Biochrom, Berlin, Germany), 100 µg/ml streptomycin (Biochrom, Berlin, Germany), and 10% heat-inactivated fetal calf serum (Biochrom, Berlin, Germany).

*mRNA analysis* - We extracted RNA from Jurkat cells using peqGOLD RNAPure (Peqlab, Erlangen, Germany) according to the distributor's manual. For the reverse transcriptase (RT) reactions we used the Advantage RT-for-PCR kit (Clontech-Takara Bio Europe, Saint-Germain-en-Laye, France). PCR for human PPAR $\gamma$  and glyceraldehyde 3-phosphate dehydrogenase (GAPDH) were performed using the MasterTaq-Kit (Eppendorf, Hamburg, Germany). Sequences of the primers were as follows: PPAR $\gamma$  (Acc. No. NM138712; 613-1324), T<sub>A</sub> = 62°C: 5' - CAT GCT TGT GAA GGA TGC AAG GG - 3', T<sub>A</sub> = 62°C 3' - GGA CGC TTT CGG AAA ACC ACT GA - 5'; GAPDH (Acc. No. NM002046; 76-1083), T<sub>A</sub> = 63 °C 5'- ATGGGGAAGGTGAAGGTCGGAGT - 3'; T<sub>A</sub> = 63°C 3'- GGGTGTACCGGAGGTTCTCATT - 5'. Products were run on a 1% agarose gel followed by ethidium bromide-staining. We calculated annealing temperatures using the primer design

MOL #34371

program Oligo (Molecular Biology Insights, Cascade, CO). Controls of isolated RNA omitting RT during PCR were used to guarantee genomic DNA-free RNA preparations (data not shown).

*Measurement of mitochondrial membrane potential ( $\Delta\Psi_M$ )* - Following individual incubations, cells were loaded with 40 nM fluorochrome 3,3'-dihexyloxacarbocyanide iodide (DiOC<sub>6</sub>(3); Molecular Probes, Leiden, The Netherlands) for 15 min, after which the dye is accumulated in mitochondria containing an intact membrane potential. After indicated treatments,  $\Delta\Psi_M$  was measured by a FACSCanto flow cytometer (BD Biosciences, Heidelberg, Germany) using FACSDiva software (BD Biosciences, Heidelberg, Germany). At least 10,000 cells were accumulated for analysis. Results are expressed as percentage of total cells with  $\Delta\Psi_M$  breakdown (dead cells).

*AnnexinV-FITC/PI staining* - To determine the amount of apoptotic and necrotic cells we used an annexinV-FITC/PI-staining kit (Immunotech, Krefeld, Germany). Detection was performed as described in the distributor's manual. Following incubations,  $2 \times 10^5$  cells were labeled with 1  $\mu$ l annexinV-FITC and 2.5  $\mu$ l PI in 100  $\mu$ l binding buffer for 15 min on ice in the dark. Afterwards, 150  $\mu$ l binding buffer was added, and cell samples were analyzed immediately using a FACSCanto flow cytometer and FACSDiva software. Apoptosis was assessed when cells were annexinV-FITC single positive. AnnexinV-FITC/PI double positive cells were considered as secondary necrotic or necrotic. A minimum of 10,000 cells were analyzed.

*DAPI staining* - Jurkat cells ( $5 \times 10^5$ ) were treated as indicated. Thereafter, cells were washed by PBS and fixed in 4% paraformaldehyde for 25 min followed by a 5 min washing step in PBS. Afterwards cells were permeabilized using 0.2% Triton-X 100 and washed 2 times again with PBS. Finally, cells were stained with DAPI ( $6 \times 10^{-7}$  M) for 10 min. Detection was done by fluorescence microscopy (Zeiss, Goettingen, Germany) using AxioVision Software (Carl Zeiss MicroImaging GmbH, Goettingen, Germany).

MOL #34371

*Cytochrome c release assay* - Mitochondrial cytochrome *c* release was determined by Western blot analysis of cytosolic cytochrome *c*, as described elsewhere (Leist et al., 1998). Briefly, cells ( $4 \times 10^6$ ) were harvested by centrifugation and resuspended in 250  $\mu$ l PBS at room temperature. Next, 250  $\mu$ l of a digitonin/sucrose solution (40  $\mu$ g digitonin in 500 mM sucrose/ $4 \times 10^6$  cells) was added for 30 sec, and the samples were subsequently centrifuged at 10,000  $\times$  g for 1 min. Cytosolic supernatants (30  $\mu$ g) were subjected to SDS/PAGE (15% gels) and Western blot analysis using an anti-cytochrome *c* antibody (PharMingen, Hamburg, Germany) was performed.

*Determination of ROS production* - For the detection of intracellular produced oxidants Jurkat cells were preloaded with 10  $\mu$ M H<sub>2</sub>DCF-DA (Molecular Probes, Leiden, The Netherlands) for 1 h at 37°C. Cells were then pelleted and washed two times with PBS. Afterwards cells were incubated with indicated treatments for 2 h followed by two washing steps with PBS. Fluorescence was measured in 10,000 cells/sample by flow cytometry (FACSCanto) with excitation and emission settings of 488 and 525 nm, respectively.

*Isolation of bovine heart submitochondrial particles (SMPs)* - Submitochondrial particles were prepared from bovine heart mitochondria as described by Okun et al. (Okun et al., 1999b), but were eventually diluted in SMP-buffer containing 75 mM sodium phosphate/1 mM MgCl<sub>2</sub>/1 mM Na-EDTA, pH 7.4. The protein concentration determined by the Lowry method (Lowry et al., 1951) was 67 mg ml<sup>-1</sup>, the cytochrome *b* concentration was 34.8  $\mu$ M and the cytochrome *a/a<sub>3</sub>* concentration was 39.2  $\mu$ M.

*Determination of complex I activities* - NADH-oxidase (complex I) activity was determined in measurements with the Oxygraph-2k (Oroboros, Innsbruck, Austria). For that SMPs (33.5  $\mu$ g protein) were added to 2 ml SMP-buffer at 25°C with 0.5 mM NADH as substrate for complex I. Oxygen consumption was measured for 15 min after indicated treatments at 25°C and calculated as percentage of untreated controls (set as 100%). For the determination of NADH: ubiquinone

MOL #34371

oxidoreductase activity of SMPs (23.5  $\mu\text{g}$  protein per assay) 100  $\mu\text{M}$  DBQ (n-decylubiquinone dissolved in DMSO) and 100  $\mu\text{M}$  NADH were used as substrates. NADH-oxidation ( $\epsilon_{340-400\text{ nm}} = 6.1\text{ mM}^{-1}\text{ cm}^{-1}$ ) rates were recorded in presence of 2 mM KCN at 30 °C using a Shimadzu Multi Spec-1501 diode array spectrophotometer.

*Determination of complex II activities* - To determine succinate-oxidase activity, SMPs (67  $\mu\text{g}$  protein) were added to 2 ml SMP-buffer containing 5 mM Na-succinate as substrate for complex II. Oxygen consumption was measured at 25°C using an Oxygraph-2k system and TZDs were added cumulatively to the maximal concentrations indicated in the figure legend. For direct determination of complex II activity SMPs (67  $\mu\text{g}$  protein) were incubated in SMP-buffer containing 5 mM Na-succinate as substrate and inhibitors for complex I (1.5  $\mu\text{M}$  rotenone), complex III (3  $\mu\text{M}$  antimycin A) and complex IV (2 mM KCN) for 10 min at 25°C. Then, 2%o dichlorophenolindophenol (DCIP) was added followed by indicated treatments. Succinate dehydrogenase (complex II) catalyzes the reaction from succinate to fumarate involving electron transfer to ubiquinone. Reduced ubiquinone was reoxidized by DCIP which could be detected as reduced DCIP at 610 nm (with 750 nm as reference) using a Shimadzu Multi Spec-1501 diode array spectrophotometer.

*ATP measurement* - For ATP determination, a commercially available luciferin-luciferase assay kit (ATP Bioluminescent Assay Kit, Sigma) was used. Briefly,  $5 \times 10^5$  Jurkat cells were treated as indicated for 2 h and lysed with 100  $\mu\text{l}$  lysing buffer. ATP determination was performed according to the distributor's manual. Whole-cell ATP content was detected by running an internal standard. The cellular ATP level was converted to percentage of untreated cells (control was set as 100%).

MOL #34371

*Statistical analysis* - We used two-tailed statistical analysis to evaluate the data. Results are expressed as the mean  $\pm$ S.D. or  $\pm$ S.E. Experiments were evaluated using the Student's *t*-test. We considered *P* values  $\leq 0.05^*$  as significant.

MOL #34371

## Results

### RESULTS

*Selection of a PPAR $\gamma$  negative Jurkat subclone.* To analyze TZD effects in T cells independent from PPAR $\gamma$  we analyzed in a first set of experiments a panel of Jurkat clones from our own and other laboratories for PPAR $\gamma$  expression. As shown in Fig. 1A, second lane and Fig. 1B, first lane one subclone did not express PPAR $\gamma$  in resting conditions whereas others were PPAR $\gamma$  positive (data not shown), which is in line with previous data (Tautenhahn et al., 2003). To test whether TZD treatment will express PPAR $\gamma$  in this Jurkat subclone, we stimulated cells with 30  $\mu$ M ciglitazone for 4 h. RT-PCR revealed no PPAR $\gamma$  expression after ciglitazone treatment (Fig. 1A, third lane). However this subclone is able to express PPAR $\gamma$  mRNA following T cell activation by TPA stimulation for 15 h as shown in Fig. 1B, second lane. But since this Jurkat subclone showed no PPAR $\gamma$  expression in conditions used in this study it was referred to as Jurkat P $^-$  and represents a suitable test system to study PPAR $\gamma$ -independent effects of TZDs.

*TZDs affect mitochondrial membrane potential ( $\Delta\Psi_M$ ).* Following treatment with TZDs we analyzed the mitochondrial membrane potential ( $\Delta\Psi_M$ ) by DiOC<sub>6</sub>(3) as a first marker of cell death in Jurkat P $^-$  cells. DiOC<sub>6</sub>(3) negative cells have lost their  $\Delta\Psi_M$  and are defined as dead cells. A 4 h treatment of Jurkat P $^-$  cells with increasing concentrations (10 – 100  $\mu$ M) of ciglitazone and troglitazone provoked a fast decrease of  $\Delta\Psi_M$ . The highest concentration of ciglitazone (100  $\mu$ M) caused 55% cell death (Fig. 2, filled circles) whereas the same concentration of troglitazone induced cell death in about 40% of cells (Fig. 2, open circles). Thus, ciglitazone is more effective than troglitazone in causing cell death in Jurkat P $^-$  T cells. However, rosiglitazone showed no depolarization of  $\Delta\Psi_M$  and consequently did not alter cell viability at any concentration up to 100  $\mu$ M (Fig. 2, filled triangles).

MOL #34371

*TZDs initiate different modes of cell death.* In contrast to rosiglitazone, ciglitazone and troglitazone led to a loss of mitochondrial membrane potential  $\Delta\Psi_M$ , which represents an early event following cell death induction. To clearly define the type of cell death induced by ciglitazone and troglitazone we performed an annexinV-FITC/PI assay 4 h following treatment. As expected incubation of Jurkat P<sup>+</sup> cells with rosiglitazone (Fig. 3A, ROSI) showed no significant induction of apoptosis compared to control (Fig. 3A, ROSI 2.8% vs. control 1.9%) whereas troglitazone (Fig. 3A, TRO) caused predominantly apoptosis, thus showing 17.1% annexinV-FITC single positive cells and a minor fraction of double positive, i. e. necrotic cells. In contrast, in cells incubated for 4 h with ciglitazone we detected 27.8% annexinV-FITC/PI double positive cells (Fig. 3A, CIG) without any significant increase in annexinV-FITC single positive (Fig. 3A CIG 5.3% vs. 1.9% of Control) and thus apoptotic cells compared to the control. This finding implies a necrotic type of cell death following ciglitazone addition. The functionality of the annexinV-FITC/PI staining protocol was assured, using the classical apoptotic trigger staurosporine (Fig. 3A, STS), which showed typical apoptotic characteristics represented by annexinV-FITC single-positive cells (75.1%) and a smaller portion (17.2%) of annexinV-FITC/PI double-positive and thus secondary necrotic cells. Similar results in discriminating between necrosis and apoptosis induced by ciglitazone and troglitazone were obtained by DAPI staining (Fig. 3B). Nuclei from troglitazone-treated cells (Fig. 3B, TRO) as well as STS-treated cells (Fig. 3B, STS) showed condensed chromatin, a hallmark of apoptosis. Arrows in Fig. 3B mark apoptotic nuclei with condensed chromatin. In line with the annexinV-FITC/PI assay, nuclei of ciglitazone-treated cells (Fig. 3B, CIG) as well as rosiglitazone-treated cells (Fig. 3B, ROSI) did not reveal apoptotic criteria. Thus, data obtained from DAPI staining further support the assumption that troglitazone induces apoptosis whereas ciglitazone provokes necrosis as the underlying mechanism of cell death in Jurkat P<sup>+</sup> T cells.



MOL #34371

*In contrast to troglitazone, ciglitazone does not induce cytochrome c release.* To confirm necrosis for ciglitazone-induced cell death and apoptosis for troglitazone-induced cell death as the underlying mechanism, we analyzed cytochrome *c* release from the mitochondria to the cytosol. This is considered an early event during the apoptotic process, which should not occur during necrosis. Therefore we analyzed cytochrome *c* release at 2 and 4 h following 50  $\mu$ M troglitazone (Fig. 4A) and 50  $\mu$ M ciglitazone (Fig. 4B) treatment. We could not detect translocation of cytochrome *c* at indicated time points after ciglitazone addition (Fig. 4B, lanes 2 and 3) whereas troglitazone treatment led to release of cytochrom *c* to the cytosol starting at 2 h following treatment (Fig. 4A, lanes 2 and 3) conforming induction of apoptosis as already detected by annexinV-FITC/PI staining. STS was used as a positive control, which induced release of cytochrome *c* to the cytosol following a 4 h treatment (Fig. 4A, lane 4). Furthermore we could show that inhibition of complex I and II of respiratory chain by the combination of rotenone/TTFA also leads to cytochrome *c* release after 4 h treatment (Fig. 4B, lane 1) and therefore induces apoptosis.

*TZDs significantly induce ROS production in Jurkat P<sup>+</sup> cells.* The generation of ROS is a general mechanism contributing to induction of necrosis (Jaattela and Tschopp, 2003) and apoptosis. TZDs are known to induce ROS production in Jurkat cells (Atarod and Kehrer, 2004). Based on our finding that TZDs induce different modes of cell death we compared relative ROS production provoked by ciglitazone, troglitazone and rosiglitazone (Fig. 5). All tested TZDs significantly induced ROS production compared to DMSO treated control. Among the tested TZDs troglitazone was the strongest inductor of ROS production (Fig. 5, column 3) whereas ciglitazone and rosiglitazone produced equal amounts of ROS (Fig. 5, columns 2 and 4). Since disruption of respiratory chain is known as an important inductor of ROS production by mitochondria

MOL #34371

(Pelicano et al., 2003) inhibition of complex I and II by their specific inhibitors rotenone and TTFA served as the positive control which led to strong ROS production (Fig. 5, column 5).

*Ciglitazone-mediated necrosis is ROS and hydrogen peroxide dependent whereas troglitazone-induced apoptosis is only partially mediated by ROS production.* To investigate the role of TZD induced ROS (Fig. 5) as a potential mediator of necrosis following ciglitazone and apoptosis following troglitazone treatment in Jurkat P<sup>+</sup> T cells we preincubated the cells using different scavengers of ROS for 2 h (Fig. 6). Preincubation with 5 mM NAC (Fig. 6A, column 2) showed no inhibitory effect on ciglitazone-provoked necrosis (set as 100% (Fig. 6A, column 1). In contrast preincubation of the cells with 300  $\mu$ M vitamin c could inhibit ciglitazone-mediated necrosis by about 40% (Fig. 6A, column 3) and 100  $\mu$ M MnTBAP (manganese (III) tetrakis (4-benzoic acid) porphyrin) which is a superoxid dismutase mimetic previously described as an effective inhibitor of ROS generation in Jurkat cells (Dolgachev et al., 2003; Hildeman et al., 1999; Huang et al., 2003; Kwon et al., 2003) by about 30% (Fig. 6A, column 5). Furthermore we suggest hydrogen peroxide as another important mediator of ciglitazone-mediated necrosis since preincubation of cells with 100 U catalase inhibited induction of necrosis by about 35% (Fig. 6A, column 4). This documented the role of ROS and hydrogen peroxide as likely mediators of ciglitazone-induced necrosis in Jurkat P<sup>+</sup> T cells.

Troglitazone-induced apoptosis was not inhibited by 2 h preincubation with 5 mM NAC (Fig. 6B, columns 2) compared to troglitazone-treated cells alone (set as 100% Fig. 6B, column 1) whereas 300  $\mu$ M vitamin c as well as 100  $\mu$ M MnTBAP reduced apoptosis by about 20% each (Fig. 6B, columns 3 and 5). Therefore ROS production is involved in troglitazone-induced apoptosis in Jurkat P<sup>+</sup> cells although it plays a minor role compared to ciglitazone-induced necrosis. Preincubation of the cells with 100 U catalase showed no significant effect (Fig. 6B, column 4) suggesting that hydrogen peroxide plays no significant role in troglitazone-induced apoptosis.

MOL #34371

*TZDs inhibit complex I of the mitochondrial respiratory chain.* Due to the fast depolarization of mitochondrial membrane potential by TZDs (Fig. 2) and the involvement of TZD evoked ROS (Fig. 5) as a cell death trigger following ciglitazone and troglitazone treatment (Fig. 6), we studied direct effects of ciglitazone, troglitazone and rosiglitazone on the mitochondrial respiratory chain using SMPs as a model system. At first we corroborated TZD effects on NADH linked respiration (Fig. 7A). Therefore, we initiated respiration in SMPs using NADH as complex I substrate. Basal respiration of untreated controls ( $0.92 \mu\text{mol O min}^{-1} \text{mg}^{-1}$ ) was set as 100%. We incubated SMPs with increasing concentrations (1 - 30  $\mu\text{M}$ ) of ciglitazone, troglitazone, rosiglitazone (Fig. 7A, ciglitazone filled circles, troglitazone open circles, rosiglitazone filled triangles) or DMSO as solvent control (data not shown) and analyzed oxygen consumption using an oxygraph. We identified a concentration-dependent inhibition of respiration with all tested TZDs. Nearly complete inhibition of respiration was detected following incubations with concentrations higher than 10  $\mu\text{M}$  ciglitazone or troglitazone (Fig. 7A), whereas rosiglitazone inhibited respiration by 80% at 30  $\mu\text{M}$ . Since succinate-linked respiration is not affected by rosiglitazone and only affected by higher concentrations of ciglitazone or troglitazone (see below), an effect of TZDs on complex I of the respiratory chain is likely, which is in line with previous studies (Brunmair et al., 2004; Scatena et al., 2004). To verify these findings, we investigated the effect of the three TZDs on the complex I specific NADH:DBQ activity (Fig. 7B). All three TZDs inhibited the NADH:DBQ activity (basal rate  $0.67 \mu\text{mol min}^{-1} \text{mg}^{-1}$ ) with the declining potency ciglitazone > troglitazone > rosiglitazone. Compared to the inhibition of the NADH-oxidase, higher concentrations were needed to block NADH:DBQ activity. This difference that was biggest in the case of rosiglitazone could be explained by direct competition with the substrate ubiquinone (DBQ) present in higher concentrations in the complex I activity test and might have been due to the specific properties of the binding domain. It is known that

MOL #34371

complex I has a relatively large ubiquinone binding pocket containing at least three overlapping binding sites for different classes of inhibitors (Okun et al., 1999a). In the NADH-oxidase measurements rosiglitazone might have effectively blocked access for the much larger and highly hydrophobic intrinsic substrate Q<sub>10</sub> while the smaller and more hydrophilic ubiquinone derivative DBQ used in the NADH:DBQ oxidoreductase assay could still enter the quinone reduction site to some extent.

*TZDs differently affect complex II of the mitochondrial respiratory chain.* We then focused on complex II (Fig. 8) by starting respiration in SMPs using Na-succinate as the complex II substrate. Basal respiration ( $0.31 \mu\text{mol O min}^{-1} \text{mg}^{-1}$ ) of untreated controls was set as 100%. We incubated SMPs with increasing concentrations (1 - 30  $\mu\text{M}$ ) of ciglitazone, troglitazone, rosiglitazone (Fig. 8A) or DMSO (data not shown) as solvent control and followed oxygen consumption using an oxygraph. In contrast to rosiglitazone (Fig. 8A), which did not inhibit respiration initiated at complex II, ciglitazone and troglitazone dose-dependently attenuated respiration. 30  $\mu\text{M}$  ciglitazone inhibited complex II initiated respiration by 70% while 30  $\mu\text{M}$  troglitazone reduced it by 40% only (Fig. 8A). Additionally, we studied effects of TZDs on the succinate:ubiquinone oxidoreductase activity of complex II in SMPs (Fig. 8B) as described under “Experimental Procedures”. The uninhibited rate of DCIP reduction ( $0.028 \mu\text{mol min}^{-1} \text{mg}^{-1}$ ) was only about 10 % of the rate of the succinate oxidase. Higher TZD concentrations were required to inhibit complex II activity compared to relative respiration. However, exposing SMPs to increasing concentrations (30 -100  $\mu\text{M}$ ) of ciglitazone and troglitazone caused a dose-dependent inhibition of complex II. The maximal effect of nearly 50% inhibition was seen at 100  $\mu\text{M}$  as the highest tested TZD concentration (Fig. 8B). Consistent with results from complex II initiated respiration (Fig. 8A), rosiglitazone did not alter complex II activity (Fig. 8B). In summary, we

MOL #34371

identified ciglitazone and troglitazone as complex II inhibitors whereas rosiglitazone did not affect complex II activity.

*Inhibition of complex II by the synthetic inhibitor TTFA rapidly induces apoptosis in Jurkat P<sup>+</sup> cells.* Based on the results using the SMP model, we investigated the influence of mitochondrial respiration chain inhibition on cell death in Jurkat P<sup>+</sup> cells. Therefore we used the established synthetic inhibitors rotenone for complex I and TTFA for complex II of the respiratory chain (Fig. 9). In control experiments, these inhibitors were tested in SMPs to confirm their functionality and specificity as complex I and II inhibitors (data not shown). Using DiOC<sub>6</sub>(3) staining we found that inhibition of complex I by rotenone (Fig. 9A, column 2) only slightly induced cell death, i. e. 10% in Jurkat P<sup>+</sup> cells, whereas inhibition of complex II by TTFA significantly increased cell death up to 30% (Fig. 9A, column 3) compared to controls (Fig. 9A column 1) or rotenone-treated Jurkat P<sup>+</sup> cells. Inhibition of complex I and II by the combination of rotenone/TTFA (Fig. 9A, column 4) increased cell death to 40% compared to controls. To prove apoptosis, cells were treated for 4 h with the combination of rotenone/TTFA and analyzed by DAPI staining. As demonstrated in Fig. 9B (Rot+TTFA) we detected condensed chromatin (highlighted by arrows), pointing at apoptosis as the underlying principle for cell death.

*ATP depletion switches apoptotic to necrotic cell death.* The ATP level in cells is critical in allowing apoptosis or provoking necrosis. Therefore, we determined the ATP level in Jurkat P<sup>+</sup> T cells after incubations with ciglitazone, troglitazone and the combination of rotenone/TTFA (Fig. 10). Following a 2 h incubation with 50  $\mu$ M or 100  $\mu$ M ciglitazone (Fig. 10, columns 2 and 3) we found a significant decrease in ATP to about 60% whereas 100  $\mu$ M troglitazone (Fig. 10, column 4) did not alter the ATP level after 2 h compared to controls (Fig. 10, column 1). Inhibition of complex I and II by the combination of rotenone/TTFA (Fig. 10, column 5) did not change the ATP level compared to controls. As expected 2-deoxy-D-glucose (2-DG) (Fig. 10, column 6), an

MOL #34371

established inhibitor of glycolysis, depleted ATP to 40% compared to control cells within a 2 h incubation period.

*Combined inhibition of complex I and II along with depletion of ATP provokes a shift from apoptosis to necrosis in Jurkat P<sup>+</sup> T cells.* To study the form of cell death induced by complex I and II inhibition in combination with ATP depletion, we incubated Jurkat P<sup>+</sup> cells with the glycolysis inhibitor 2-DG and with the complex I and II inhibitors rotenone/TTFA (Fig. 11). As shown by annexinV-FITC/PI staining, rotenone/TTFA induced cell death after 4 h with typical characteristics of apoptosis as represented by mainly annexinV-FITC single positive cells (Fig. 11, Rot+TTFA, lower right 18.7%) compared to controls (Fig. 11, Control). Depletion of ATP with 2-DG alone, as already shown in Fig. 10, column 6, left cell viability unaltered (Fig. 11, 2-DG vs. control). However, 4 h coincubations of cells with 2-DG and the complex I and II inhibitors rotenone/TTFA produced a shift to annexinV-FITC/PI double positive cells (Fig. 11, 2-DG+Rot+TTFA, upper right 35.5%) pointing to necrosis as the underlying mode of cell death. Thus, depletion of ATP in Jurkat P<sup>+</sup> cells in combination with inhibition of complex I and II as the apoptotic stimuli provokes a shift from apoptosis to necrosis. These data underscore the importance of decreased ATP levels as an additional factor for ciglitazone-induced necrosis.

MOL #34371

## Discussion

### DISCUSSION

We focused on PPAR $\gamma$ -independent mechanisms of TZD induced cell death in Jurkat T cells. While ciglitazone and troglitazone inhibited complex I and complex II of the mitochondrial respiratory chain, rosiglitazone affected only complex I. Complex I and II inhibition by synthetic inhibitors or troglitazone evoked a fast induction of apoptosis. In contrast, ciglitazone induced necrosis. We identified that ciglitazone, but not troglitazone, additionally causes ATP depletion, thus explaining a shift from apoptosis to necrosis.

PPAR $\gamma$  activation by TZDs provoked T cell apoptosis (Harris and Phipps, 2000; Harris and Phipps, 2001; Harris and Phipps, 2002; Kanunfre et al., 2004; Tautenhahn et al., 2003). However, TZDs also activate cell death pathways independent of PPAR $\gamma$ . Considering that TZDs are employed as therapeutic agents, understanding PPAR $\gamma$ -dependent and -independent signaling pathways are inevitable. We concentrated on PPAR $\gamma$ -independent effects by using a Jurkat subclone lacking PPAR $\gamma$  mRNA expression under resting conditions as well as following TZD treatment (Jurkat P<sup>-</sup> subclone). Furthermore, TZD concentrations were much higher than their EC<sub>50</sub> values for PPAR $\gamma$  activation (Willson et al., 1996), therefore disregarding PPAR $\gamma$ -dependent effects.

As reported for HepG2 cells (Bova et al., 2005; Tirmenstein et al., 2002), we found that high troglitazone concentrations provoked apoptotic cell death in Jurkat P<sup>-</sup> cells. Ciglitazone elicited fast induction of cell death, which is in line with previous publications (Atarod and Kehrer, 2004; Kanunfre et al., 2004). Rosiglitazone did not alter cell viability at any concentration after 4 h, which is in agreement with data from hepatoma cells (Narayanan et al., 2003).

MOL #34371

TZD concentrations used in our study might also mimic therapeutic settings because taking AUC (area under the curve; an index of total drug exposure) concentrations into consideration (e.g. AUC for troglitazone reaches 55  $\mu$ M serum concentration (Feinstein et al., 2005)), a long time exposure to low concentrations can be as effective as shorter exposures to higher concentrations. To prove this, we incubated Jurkat P<sup>+</sup> cells with TZDs up to 10  $\mu$ M, for up to 72 h (data not shown). With FCS being reduced to 2%, at 48 h necrosis was seen with 10  $\mu$ M ciglitazone and apoptosis occurred with 10  $\mu$ M troglitazone.

Work of others pointed to mitochondria as potential targets in TZD-dependent cell death, showing complex I inhibition for several cell types (Bova et al., 2005; Brunmair et al., 2004; Dello Russo et al., 2003; Narayanan et al., 2003; Perez-Ortiz et al., 2004; Scatena et al., 2004; Tirmenstein et al., 2002). We used SMPs, representing a cell free test system, to identify the impact of TZDs on the mitochondria respiratory chain. We corroborated previous studies (Brunmair et al., 2004; Scatena et al., 2004) showing that TZDs inhibited complex I, with the discriminating rank order ciglitazone > troglitazone > rosiglitazone. Focusing on complex II of the respiratory chain, we found its inhibition by ciglitazone and troglitazone. This is in contrast to data from Scatena et al. who mentioned that ciglitazone did not alter succinate dehydrogenase and thus complex II activity in permeabilized HL-60 cells (Scatena et al., 2004). This can be explained by the different test systems (digitonin-permeabilized cells vs. SMPs) and methods used to monitor complex II activity. For a significant determination of succinate dehydrogenase activity it is necessary to use isolated mitochondria to avoid artificial reduction of electron acceptors by cytosolic enzymes as described by O'Donnell et al. (O'Donnell et al., 1995) which is given using SMPs as a test system. Our data proved different TZD concentrations to inhibit complex II as part of the succinate oxidase (which encloses the respiratory chain complexes III and IV) vs. the succinate-ubiquinone oxidoreductase activity of complex II. In the latter assay,



MOL #34371

complex II catalyzes the reduction of respiratory chain component ubiquinone, which subsequently reduces DCIP. However, DCIP reduction is neither specific nor does it quantitatively reflect ubiquinone reduction. In some measurements a background of about 10% could not be reduced by the known complex II inhibitor TTFA. Nevertheless, inhibition of complex II by ciglitazone and troglitazone was detected with both methods, whereas rosiglitazone neither effected succinate oxidase nor the succinate-ubiquinone oxidoreductase activity of complex II.

To corroborate the SMP results with our T cell model, we investigated effects on cell death in Jurkat P<sup>+</sup> cells following respiratory chain inhibition using known complex I (rotenone) and II (TTFA) inhibitors. Complex I inhibition marginally affected cell death at 4 h. This is in line with studies in HL-60 cells showing significant induction of apoptosis starting 24 h following complex I inhibition by rotenone (Li et al., 2003; Pelicano et al., 2003). Moreover, rosiglitazone, identified as a weaker complex I inhibitor in our study, failed to induce cell death after 4 h. Interestingly, inhibition of complex II by TTFA (Ingledew and Ohnishi, 1977; Zhang and Fariss, 2002) provoked significant cell death after 4 h. The importance of complex II causing rapid effects at the mitochondria was previously demonstrated in human neuroblastoma cells (Fernandez-Gomez et al., 2005), when the complex II inhibitor malonate provoked a fast mitochondrial depolarization. This supports our finding that ciglitazone- and troglitazone-dependent complex II inhibition instantaneously induced cell death. Because ciglitazone and troglitazone also inhibit complex I activity, we analyzed cell death induction following combined inhibition of complex I and II by rotenone/TTFA. We identified a further increase of cell death compared to inhibition of complex II by TTFA only. This suggests that TZD-dependent inhibition of complex I and II overlaps to immediately provoke apoptosis. This explains induction of apoptosis following troglitazone treatment but does not rationalize induction of necrosis by ciglitazone. Previous

MOL #34371

studies in Jurkat cells by Leist et al. demonstrated that intracellular ATP levels decide between apoptosis or necrosis following an apoptotic trigger (Leist et al., 1997). They suggest that ATP depletion in combination with an apoptotic stimulus initiates a switch from apoptosis to necrosis. Recently, a concentration- and time-dependent ATP depletion following ciglitazone treatment was found in explanted Sprague-Dawley rat lenses (Aleo et al., 2005), while we observed ATP depletion in Jurkat P<sup>+</sup> cells. In line with reports in rat hepatocytes (Haskins et al., 2001), troglitazone and the combination of rotenone/TTFA did not significantly reduce the ATP content. Inhibition of complexes I and II with rotenone/TTFA in combination with ATP depletion by 2-DG switches apoptosis to necrosis, supporting our hypothesis that inhibition of complexes I and II along with ATP depletion by ciglitazone initiated necrosis, whereas troglitazone, leaving the ATP content unaltered, caused apoptosis. However, the mechanisms provoking ciglitazone-mediated ATP depletion remains unclear.

Inhibition of mitochondrial respiration provoked increased ROS production (Pelicano et al., 2003), which we identified as a potential inducer of necrosis following ciglitazone treatment due to cytoprotective effects of vitamin c and MnTBAP. We also noticed an inhibitory effect of catalase, which is not able to pass the cell membrane, assuming that hydrogen peroxide in the medium plays a contributing role. The efficacy of catalase was confirmed by blocking hydrogen peroxide-induced cell death in Jurkat P<sup>+</sup> cells (data not shown). We suggest that ciglitazone provokes ROS production, including hydrogen peroxide, which contributes to necrosis induction in neighbouring cells. This data is in contrast to the report of Atarod et al. (Atarod and Kehrer, 2004), showing no protection by vitamin c or catalase, while MnTBAP has not been tested in their study. They used higher concentrations of ciglitazone and vitamin c which might explain the differences. Moreover, necrosis induced by ciglitazone was not completely inhibited by MnTBAP, vitamin c or catalase. Therefore, we propose that ROS and hydrogen contribute to cell

MOL #34371

death induction. Troglitazone-induced apoptosis was also inhibited by vitamin c and MnTBAP, although protection was weaker than observed for ciglitazone-induced necrosis. Likely, ROS are not the only trigger for troglitazone-induced apoptosis. Since rosiglitazone inhibits complex I of the respiratory chain we expected production of ROS. However, no significant cell death was observed after 4 h treatment, which may be due to culture conditions (10% vs. 2% FCS) as already mentioned. ROS production not necessarily induces apoptosis as shown by Atarod et al. (Atarod and Kehrer, 2004), when the PPAR $\alpha$  agonist WY14643 significantly increases ROS without affecting cell survival even after treatment with 100  $\mu$ M for up to 48 h. Therefore, we suggest that TZD evoked ROS contribute to cell death, whereas inhibition of complex II by ciglitazone and troglitazone is the main trigger of cell death. However, the mechanism of cell death induction by inhibition of complex II is still unknown.

Our data suggest that despite their similar structure TZDs affect cell death by different mechanisms, provoking apoptosis or necrosis. Since TZDs are discussed as potential therapeutic agents for the treatment of cancer, various inflammatory and neurodegenerative diseases (Pershadsingh, 2004), beside their current use for the treatment of diabetes type 2, the mechanisms explored in this study may help to understand possible adverse effects occurring during TZD-based therapies.

MOL #34371

## **Acknowledgements**

### **ACKNOWLEDGEMENTS**

We thank Ilka Siebels for excellent technical assistance.

MOL #34371

## References

## REFERENCES

- Aleo MD, Doshna CM and Navetta KA (2005) Ciglitazone-induced lenticular opacities in rats: in vivo and whole lens explant culture evaluation. *J Pharmacol Exp Ther* **312**:1027-1033.
- Atarod EB and Kehrer JP (2004) Dissociation of oxidant production by peroxisome proliferator-activated receptor ligands from cell death in human cell lines. *Free Radic Biol Med* **37**:36-47.
- Bova MP, Tam D, McMahon G and Mattson MN (2005) Troglitazone induces a rapid drop of mitochondrial membrane potential in liver HepG2 cells. *Toxicol Lett* **155**:41-50.
- Brunmair B, Staniek K, Gras F, Scharf N, Althaym A, Clara R, Roden M, Gnaiger E, Nohl H, Waldhausl W and Fornsinn C (2004) Thiazolidinediones, like metformin, inhibit respiratory complex I: a common mechanism contributing to their antidiabetic actions? *Diabetes* **53**:1052-1059.
- Daynes RA and Jones DC (2002) Emerging roles of PPARs in inflammation and immunity. *Nat Rev Immunol* **2**:748-759.
- Dello Russo C, Gavriluk V, Weinberg G, Almeida A, Bolanos JP, Palmer J, Pelligrino D, Galea E and Feinstein DL (2003) Peroxisome proliferator-activated receptor gamma thiazolidinedione agonists increase glucose metabolism in astrocytes. *J Biol Chem* **278**:5828-5836.
- Dolgachev V, Nagy B, Taffe B, Hanada K and Separovic D (2003) Reactive oxygen species generation is independent of de novo sphingolipids in apoptotic photosensitized cells. *Exp Cell Res* **288**:425-436.
- Feinstein DL, Spagnolo A, Akar C, Weinberg G, Murphy P, Gavriluk V and Russo CD (2005) Receptor-independent actions of PPAR thiazolidinedione agonists: is mitochondrial function the key? *Biochem Pharmacol* **70**:177-188.
- Fernandez-Gomez FJ, Galindo MF, Gomez-Lazaro M, Yuste VJ, Comella JX, Aguirre N and Jordan J (2005) Malonate induces cell death via mitochondrial potential collapse and delayed swelling through an ROS-dependent pathway. *Br J Pharmacol* **144**:528-537.
- Harris SG and Phipps RP (2000) Peroxisome proliferator-activated receptor gamma (PPAR-gamma) activation in naive mouse T cells induces cell death. *Ann N Y Acad Sci* **905**:297-300.
- Harris SG and Phipps RP (2001) The nuclear receptor PPAR gamma is expressed by mouse T lymphocytes and PPAR gamma agonists induce apoptosis. *Eur J Immunol* **31**:1098-1105.
- Harris SG and Phipps RP (2002) Induction of apoptosis in mouse T cells upon peroxisome proliferator-activated receptor gamma (PPAR-gamma) binding. *Adv Exp Med Biol* **507**:421-425.
- Haskins JR, Rowse P, Rahbari R and de la Iglesia FA (2001) Thiazolidinedione toxicity to isolated hepatocytes revealed by coherent multiprobe fluorescence microscopy and correlated with multiparameter flow cytometry of peripheral leukocytes. *Arch Toxicol* **75**:425-438.
- Hildeman DA, Mitchell T, Teague TK, Henson P, Day BJ, Kappler J and Marrack PC (1999) Reactive oxygen species regulate activation-induced T cell apoptosis. *Immunity* **10**:735-744.

MOL #34371

- Huang HL, Fang LW, Lu SP, Chou CK, Luh TY and Lai MZ (2003) DNA-damaging reagents induce apoptosis through reactive oxygen species-dependent Fas aggregation. *Oncogene* **22**:8168-8177.
- Ingledeu WJ and Ohnishi T (1977) The probable site of action of thenolytrifluoroacetone on the respiratory chain. *Biochem J* **164**:617-620.
- Jaattela M and Tschopp J (2003) Caspase-independent cell death in T lymphocytes. *Nat Immunol* **4**:416-423.
- Kanunfre CC, da Silva Freitas JJ, Pompeia C, Goncalves de Almeida DC, Cury-Boaventura MF, Verlengia R and Curi R (2004) Ciglitazone and 15d PGJ2 induce apoptosis in Jurkat and Raji cells. *Int Immunopharmacol* **4**:1171-1185.
- Kersten S, Desvergne B and Wahli W (2000) Roles of PPARs in health and disease. *Nature* **405**:421-424.
- Kwon J, Devadas S and Williams MS (2003) T cell receptor-stimulated generation of hydrogen peroxide inhibits MEK-ERK activation and Ick serine phosphorylation. *Free Radic Biol Med* **35**:406-417.
- Leist M, Single B, Castoldi AF, Kühnle S and Nicotera P (1997) Intracellular adenosine triphosphate (ATP) concentration: a switch in the decision between apoptosis and necrosis. *J Exp Med* **185**:1481-1486.
- Leist M, Volbracht C, Fava E and Nicotera P (1998) 1-Methyl-4-phenylpyridinium induces autocrine excitotoxicity, protease activation, and neuronal apoptosis. *Mol Pharmacol* **54**:789-801.
- Li N, Ragheb K, Lawler G, Sturgis J, Rajwa B, Melendez JA and Robinson JP (2003) Mitochondrial complex I inhibitor rotenone induces apoptosis through enhancing mitochondrial reactive oxygen species production. *J Biol Chem* **278**:8516-8525.
- Lowry OH, Rosebrough NJ, Farr AL and Randall RJ (1951) Protein measurement with the Folin phenol reagent. *J Biol Chem* **193**:265-275.
- Narayanan PK, Hart T, Elcock F, Zhang C, Hahn L, McFarland D, Schwartz L, Morgan DG and Bugelski P (2003) Troglitazone-induced intracellular oxidative stress in rat hepatoma cells: a flow cytometric assessment. *Cytometry A* **52**:28-35.
- O'Donnell VB, Spycher S and Azzi A (1995) Involvement of oxidants and oxidant-generating enzyme(s) in tumour-necrosis-factor- $\alpha$ -mediated apoptosis: role for lipoxygenase pathway but not mitochondrial respiratory chain. *Biochem J* **310** ( Pt 1):133-141.
- Okun JG, Lummen P and Brandt U (1999a) Three classes of inhibitors share a common binding domain in mitochondrial complex I (NADH:ubiquinone oxidoreductase). *J Biol Chem* **274**:2625-2630.
- Okun JG, Zickermann V and Brandt U (1999b) Properties of the common inhibitor-binding domain in mitochondrial NADH-dehydrogenase (complex I). *Biochem Soc Trans* **27**:596-601.
- Pelicano H, Feng L, Zhou Y, Carew JS, Hileman EO, Plunkett W, Keating MJ and Huang P (2003) Inhibition of mitochondrial respiration: a novel strategy to enhance drug-induced apoptosis in human leukemia cells by a reactive oxygen species-mediated mechanism. *J Biol Chem* **278**:37832-37839.
- Perez-Ortiz JM, Tranque P, Vaquero CF, Domingo B, Molina F, Calvo S, Jordan J, Cena V and Llopis J (2004) Glitazones differentially regulate primary astrocyte and glioma cell survival. Involvement of reactive oxygen species and peroxisome proliferator-activated receptor- $\gamma$ . *J Biol Chem* **279**:8976-8985.

MOL #34371

- Pershadsingh HA (2004) Peroxisome proliferator-activated receptor-gamma: therapeutic target for diseases beyond diabetes: quo vadis? *Expert Opin Investig Drugs* **13**:215-228.
- Rybczynski PJ, Zeck RE, Combs DW, Turchi I, Burris TP, Xu JZ, Yang M and Demarest KT (2003) Benzoxazinones as PPARgamma agonists. part 1: SAR of three aromatic regions. *Bioorg Med Chem Lett* **13**:2359-2362.
- Scatena R, Bottoni P, Martorana GE, Ferrari F, De Sole P, Rossi C and Giardina B (2004) Mitochondrial respiratory chain dysfunction, a non-receptor-mediated effect of synthetic PPAR-ligands: biochemical and pharmacological implications. *Biochem Biophys Res Commun* **319**:967-973.
- Soller M, Tautenhahn A, Brune B, Zacharowski K, John S, Link H and von Knethen A (2006) Peroxisome proliferator-activated receptor gamma contributes to T lymphocyte apoptosis during sepsis. *J Leukoc Biol* **79**:235-243.
- Tautenhahn A, Brune B and von Knethen A (2003) Activation-induced PPARgamma expression sensitizes primary human T cells toward apoptosis. *J Leukoc Biol* **73**:665-672.
- Tirmenstein MA, Hu CX, Gales TL, Maleeff BE, Narayanan PK, Kurali E, Hart TK, Thomas HC and Schwartz LW (2002) Effects of troglitazone on HepG2 viability and mitochondrial function. *Toxicol Sci* **69**:131-138.
- Tolman KG (2000) Thiazolidinedione hepatotoxicity: a class effect? *Int J Clin Pract Suppl*:29-34.
- Willson TM, Cobb JE, Cowan DJ, Wiethe RW, Correa ID, Prakash SR, Beck KD, Moore LB, Kliewer SA and Lehmann JM (1996) The structure-activity relationship between peroxisome proliferator-activated receptor gamma agonism and the antihyperglycemic activity of thiazolidinediones. *J Med Chem* **39**:665-668.
- Zhang JG and Fariss MW (2002) Thenoyltrifluoroacetone, a potent inhibitor of carboxylesterase activity. *Biochem Pharmacol* **63**:751-754.

MOL #34371

## Footnotes

---

<sup>⊥</sup>The work was supported by grants from Deutsche Forschungsgemeinschaft (BR999),  
Krebshilfe and Sander Foundation.

Address of correspondence: Andreas von Knethen, Department of Biochemistry I -  
Pathobiochemistry, Johann Wolfgang Goethe-University, Faculty of Medicine, Theodor-Stern-  
Kai 7, 60590 Frankfurt/Main, Germany, Phone: +49-69-6301 6989; Fax: +49-69-6301 4203; E-  
Mail: v\_knethen@zbc.kgu.de



MOL #34371

## Legends for figures

### FIGURE LEGENDS

Fig. 1. PPAR $\gamma$  mRNA expression in Jurkat cells. Jurkat cells were treated A, with 30  $\mu$ M ciglitazone for 4 h or B, with 25 nM TPA for 15 h or remained as controls, followed by RT-PCR analysis for PPAR $\gamma$  and GAPDH as described under “Experimental Procedures”. A, Agarose gel electrophoresis shows PCR products for PPAR $\gamma$  and GAPDH from untreated (second lane) and ciglitazone treated (third lane) Jurkat cells and a 1kb DNA ladder (M) in the first lane. The fourth lane (C<sup>+</sup>) shows the PCR product obtained from a plasmid containing full PPAR $\gamma$ . B, PPAR $\gamma$  and GAPDH PCR products from untreated cells (first lane) and TPA treated cells (second lane) as well as a 1kb DNA ladder (third lane) is shown. Data are representative of three separate RT-PCR analyses.

Fig. 2. TZD-induced cell death in Jurkat P<sup>+</sup> cells. Jurkat P<sup>+</sup> cells were treated with increasing concentrations of ciglitazone, troglitazone and rosiglitazone from 10 to 100  $\mu$ M for 4 h. Survival of cells was analyzed by flow cytometry using DiOC<sub>6</sub>(3) as described in “Experimental Procedures”. Cell death is expressed as percent DiOC<sub>6</sub>(3) negative cells of whole cell population. Values are means  $\pm$  S.E., n = 12.

Fig. 3. Characterization of cell death induction by ciglitazone and troglitazone. Jurkat P<sup>+</sup> cells were treated with 0.5  $\mu$ g/ml staurosporine (STS) as an established inducer of apoptosis, 50  $\mu$ M ciglitazone (CIG), 100  $\mu$ M troglitazone (TRO) and 100  $\mu$ M rosiglitazone (ROSI) or left untreated (Control) for 4 h. A, cells were collected, washed, followed by annexinV-FITC/PI staining to distinguish apoptosis vs. necrosis using flow cytometry as described in “Experimental

MOL #34371

Procedures". Data are representatives of three separate experiments. *B*, representative images of DAPI stained untreated, STS, CIG, TRO and ROSI incubated Jurkat P<sup>+</sup> cells detected by fluorescence microscopy as described in "Experimental Procedures". Arrows mark cells with condensed chromatin. Magnification 400x.

Fig. 4. Troglitazone induces cytochrome *c* release whereas ciglitazone-mediated cell death is unrelated to cytochrome *c* release. Jurkat P<sup>+</sup> cells were incubated with *A*, 50  $\mu$ M troglitazone and staurosporine 0.5  $\mu$ g/ml (STS) as a classical inducer of apoptosis or *B*, 50  $\mu$ M ciglitazone as well as the combination rotenone (inhibitor of complex I) 25  $\mu$ M/TTFA (inhibitor of complex II) 200  $\mu$ M for times indicated or remained as controls. Cytosolic cytochrome *c* vs. mitochondrial cytochrome *c* were determined by immunoblot analysis as described under "Experimental Procedures". One representative blot out of three is shown.

Fig. 5. TZDs provoke the production of ROS in Jurkat P<sup>+</sup> cells. H<sub>2</sub>DCF-DA stained cells were incubated with ciglitazone, troglitazone and rosiglitazone each at 50  $\mu$ M as well as the combination of rotenone 25  $\mu$ M and TTFA 200  $\mu$ M for 2 h or DMSO as control. ROS were determined using H<sub>2</sub>DCF-DA staining as described in "Experimental Procedures". Data are means  $\pm$  S.E., n = 6, \*\**p* < 0.01.

Fig. 6. Ciglitazone-induced necrosis in Jurkat P<sup>+</sup> cells is ROS- and hydrogen peroxide- dependent whereas troglitazone provoked apoptosis is only partially induced by ROS. Jurkat P<sup>+</sup> cells were preincubated for 2 h with 5 mM NAC, 300  $\mu$ M Vit c, 100 U catalase or 100  $\mu$ M of the SOD mimetic MnTBAP prior to treatment for 4 h with *A*, 50  $\mu$ M ciglitazone or *B*, 50  $\mu$ M troglitazone.

MOL #34371

Cells were washed and stained with DiOC<sub>6</sub>(3). Percentage of DiOC<sub>6</sub>(3) negative cells were estimated using flow cytometry as described in “Experimental Procedures”. Inhibition of cell death by ROS scavengers is expressed as percentage of ciglitazone- or troglitazone- induced cell death set as 100%. Data are means  $\pm$  S.E., n = 8, \**p* < 0.05, \*\*\**p* < 0.001.

Fig. 7. TZDs inhibit complex I of the mitochondrial respiratory chain. SMPs were prepared as described under “Experimental Procedures” and incubated with increasing concentrations (1 - 250  $\mu$ M) of ciglitazone, troglitazone and rosiglitazone. *A*, Respiration in SMPs was initiated by NADH (complex I substrate) and oxygen consumption was detected by an oxygraph-2K system. Level of respiration was calculated as percentage of controls. Data are means  $\pm$  S.D., n = 3. *B*, effect of TZDs on the NADH:DBQ activity of SMPs. The NADH:DBQ activity was determined as described under “Experimental Procedures” and related to the uninhibited rate (0.67  $\mu$ mol min<sup>-1</sup> mg<sup>-1</sup>) of NADH-oxidation. Each point represents the mean value  $\pm$  S.D. of 3 independent measurements.

Fig. 8. Ciglitazone and troglitazone inhibit complex II of the mitochondrial respiratory chain. SMPs were prepared as described under “Experimental Procedures” and after addition of the complex II substrate Na-succinate incubated with increasing concentrations (1 – 100  $\mu$ M) of ciglitazone, troglitazone and rosiglitazone. *A*, respiration in SMPs was detected by measuring oxygen consumption by an oxograph-2K system and calculated as percentage of controls. Data are means  $\pm$  S.D., n = 3. *B*, direct complex II activity was detected as described under “Experimental Procedures” following increasing concentrations of TZDs. Data are means  $\pm$  S.D., n = 3.

MOL #34371

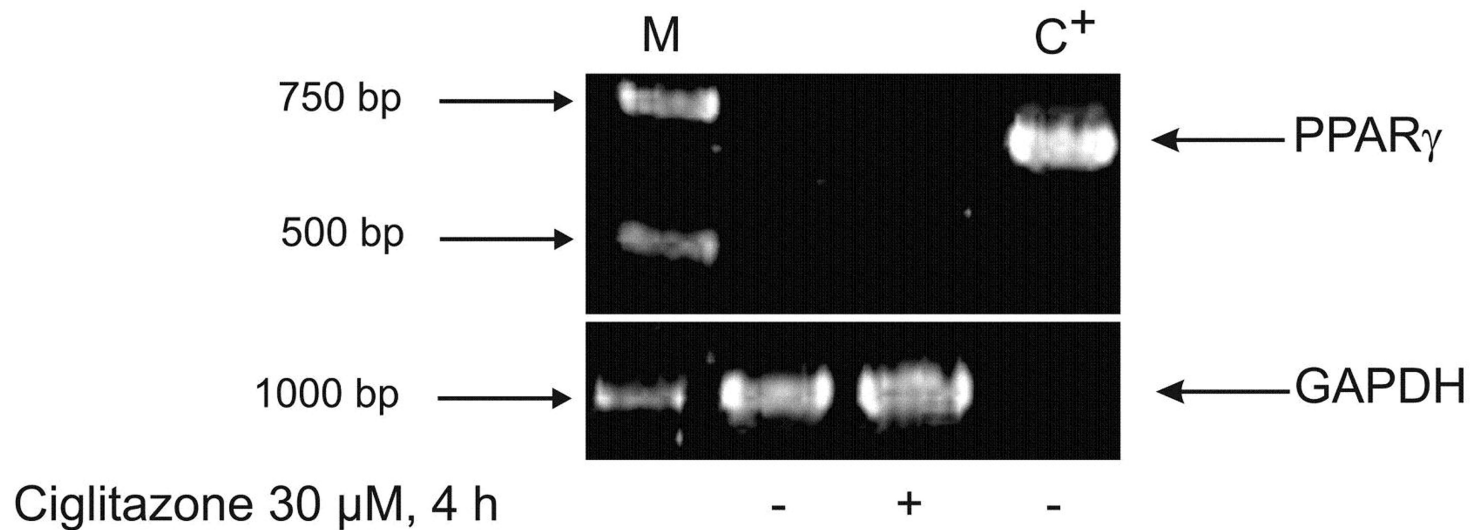
Fig. 9. Inhibition of complex I and II of the respiratory chain provoked apoptosis. Cells were incubated with 25  $\mu$ M rotenone (inhibitor complex I), 200  $\mu$ M TTFA (inhibitor complex II), rotenone/TTFA in combination or remained as controls. *A*, following incubations for 4 h cell death was detected by flow cytometry using DiOC<sub>6</sub>(3) staining as described in “Experimental Procedures”. Cell death is represented as percentage of DiOC<sub>6</sub>(3) negative cells of whole cell population. Data are means  $\pm$  S.E.,  $n = 12$ ,  $**p < 0.01$ ,  $***p < 0.001$ . *B*, representative image of DAPI stained Jurkat P<sup>+</sup> cells treated with rotenone and TTFA as described in “Experimental Procedures”. Arrows mark condensed chromatin. Magnification 400x.

Fig. 10. Ciglitazone decreased the ATP level in Jurkat P<sup>+</sup> cells. Jurkat P<sup>+</sup> cells were incubated for 2 h with 50  $\mu$ M or 100  $\mu$ M ciglitazone, 100  $\mu$ M troglitazone, 20 mM 2-DG, the combination of 25  $\mu$ M rotenone and 200  $\mu$ M TTFA, or remained as controls. Cells were harvested and whole-cell ATP was determined as described under “Experimental Procedures”. ATP levels are given as percentage relative to untreated cells (control set as 100%). Values are means  $\pm$  S.D.,  $n = 5$ ,  $**p < 0.01$ .

Fig. 11. ATP depletion shifted apoptosis to necrosis. Jurkat P<sup>+</sup> cells were incubated with the combination 25  $\mu$ M rotenone/200  $\mu$ M TTFA, 20 mM 2-DG and the combination 2-DG + rotenone/TTFA or remained as controls. Cells were collected, washed and stained by annexinV-FITC/PI for flow cytometry as described under “Experimental Procedures”. Data are representatives of three separate experiments.

# Figure 1

A



B

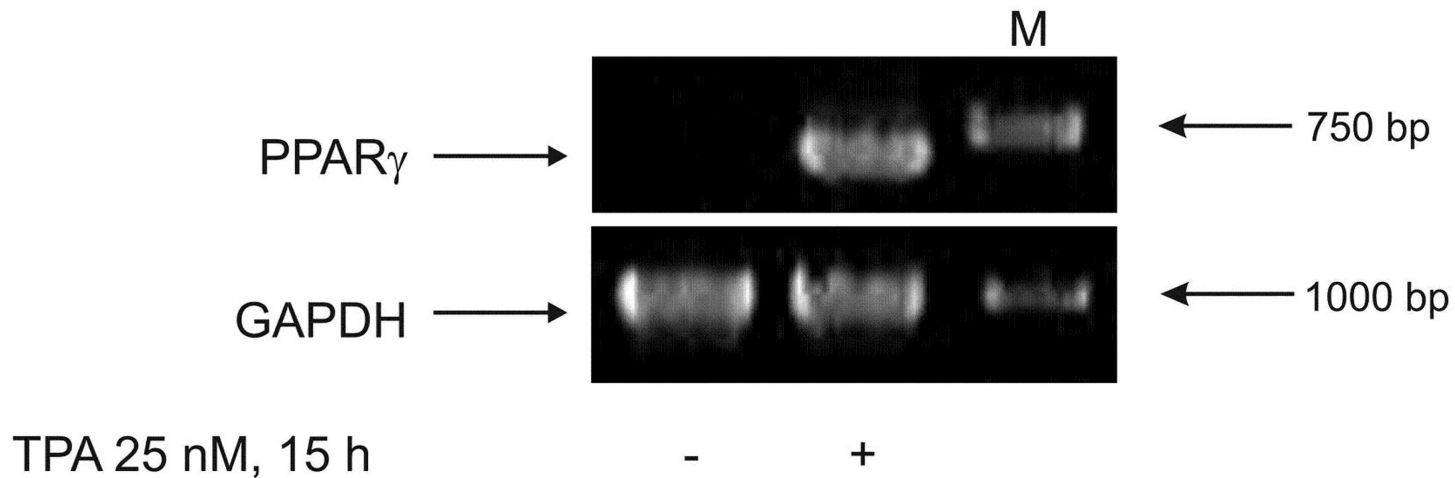
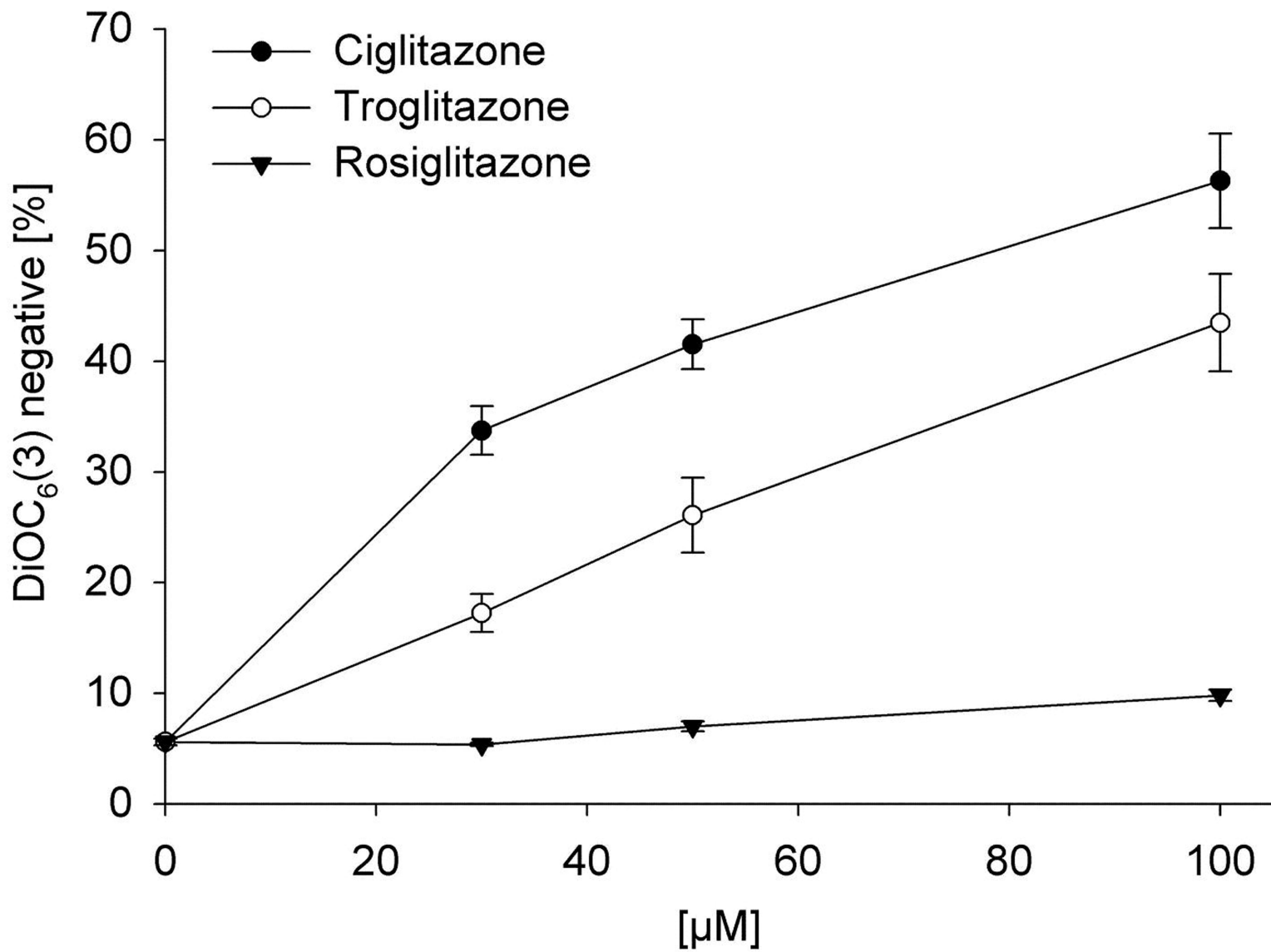
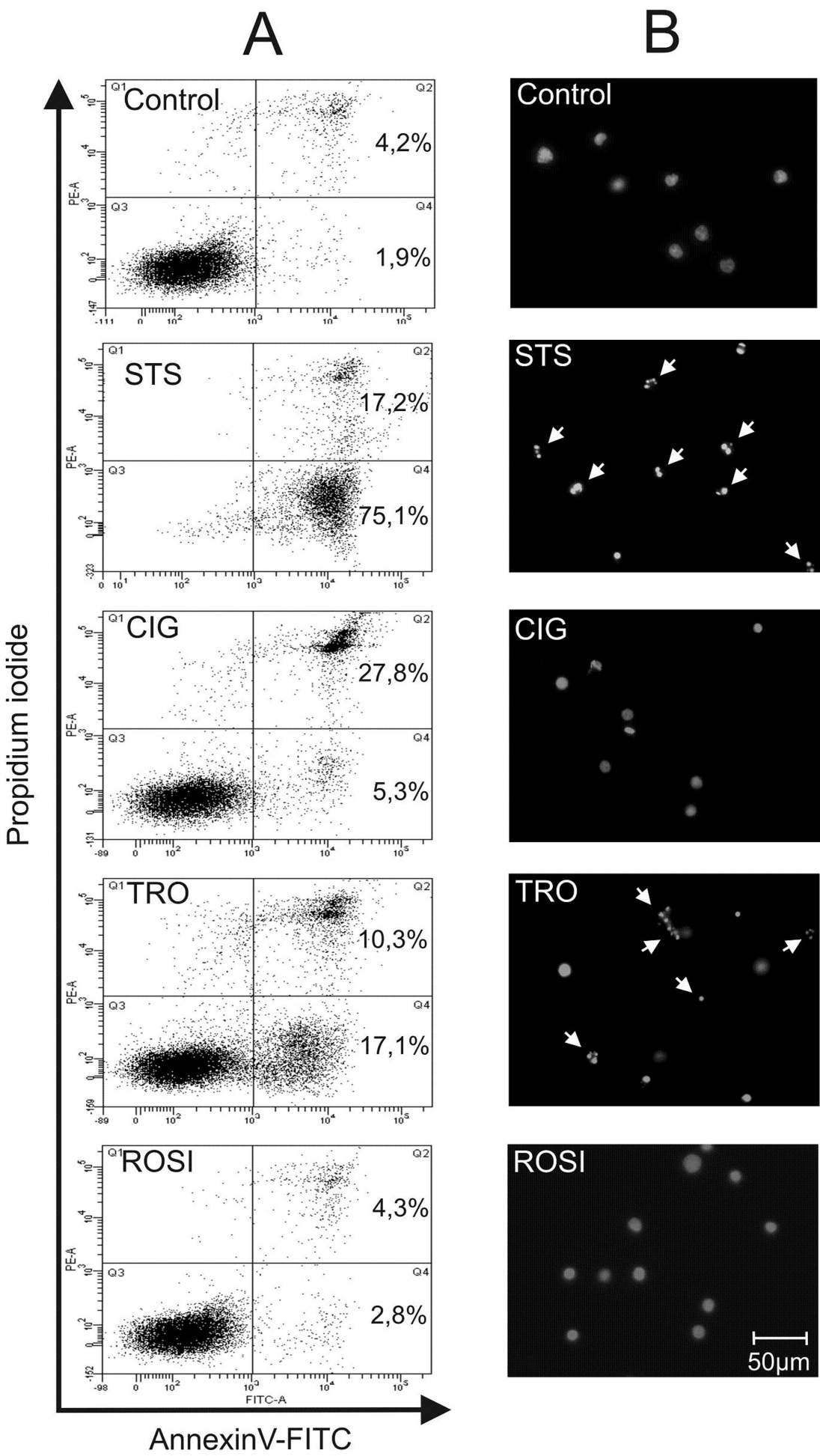


Figure 2

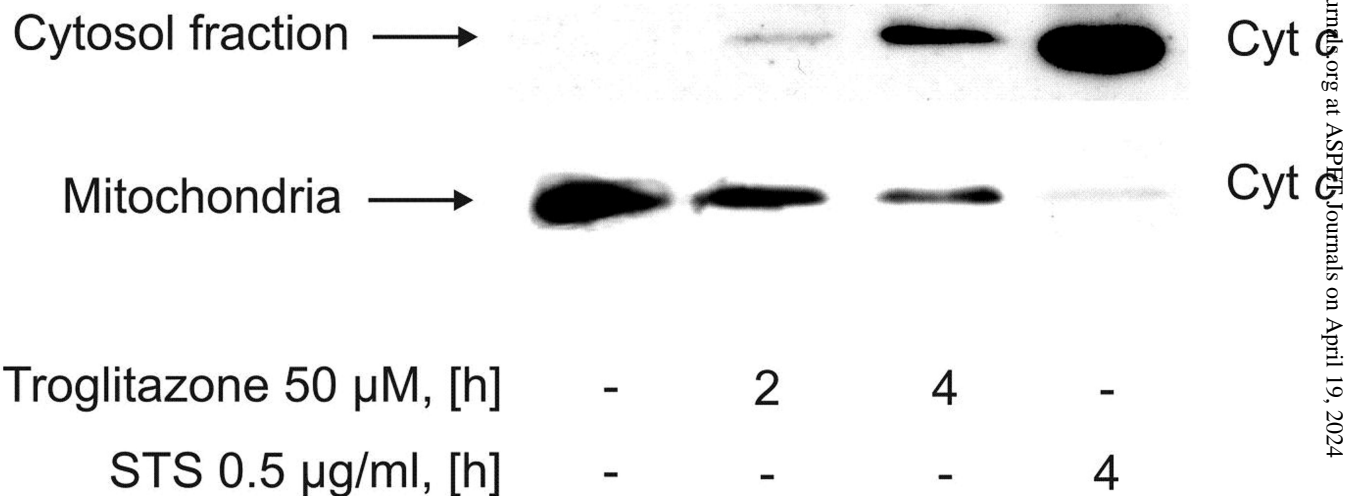


# Figure 3



# Figure 4

A



B

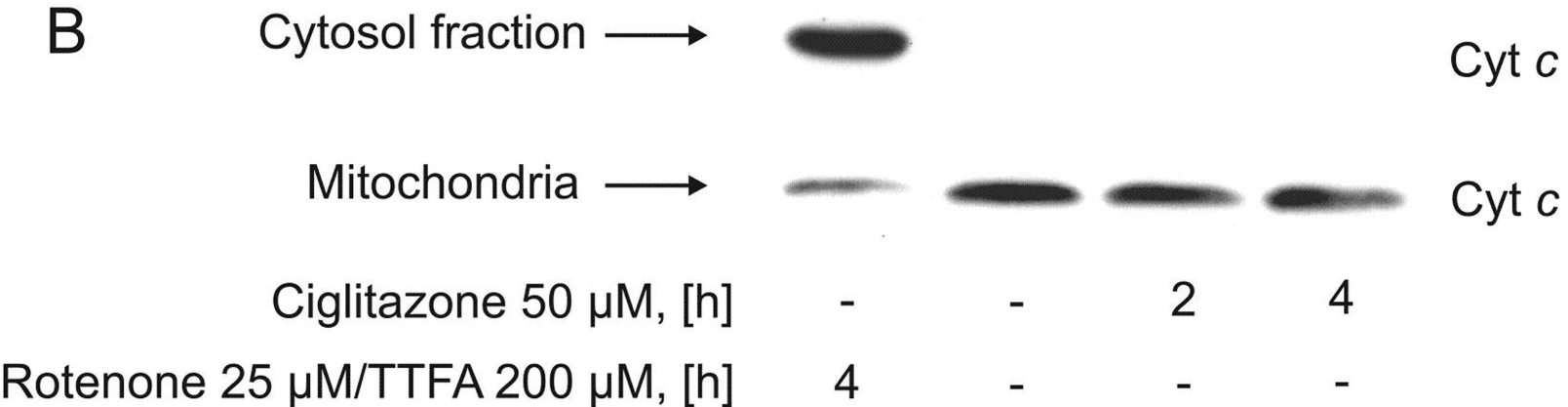
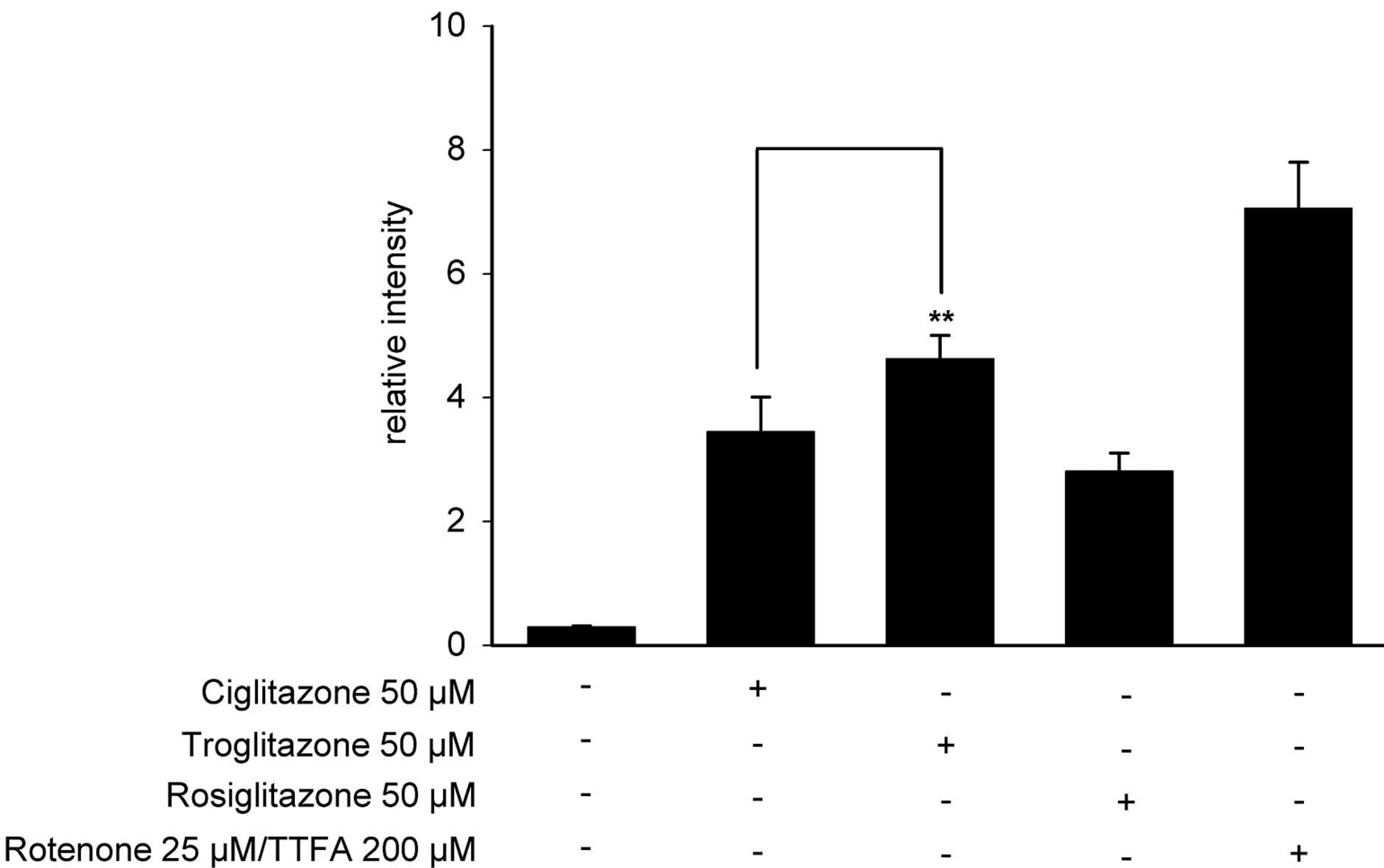


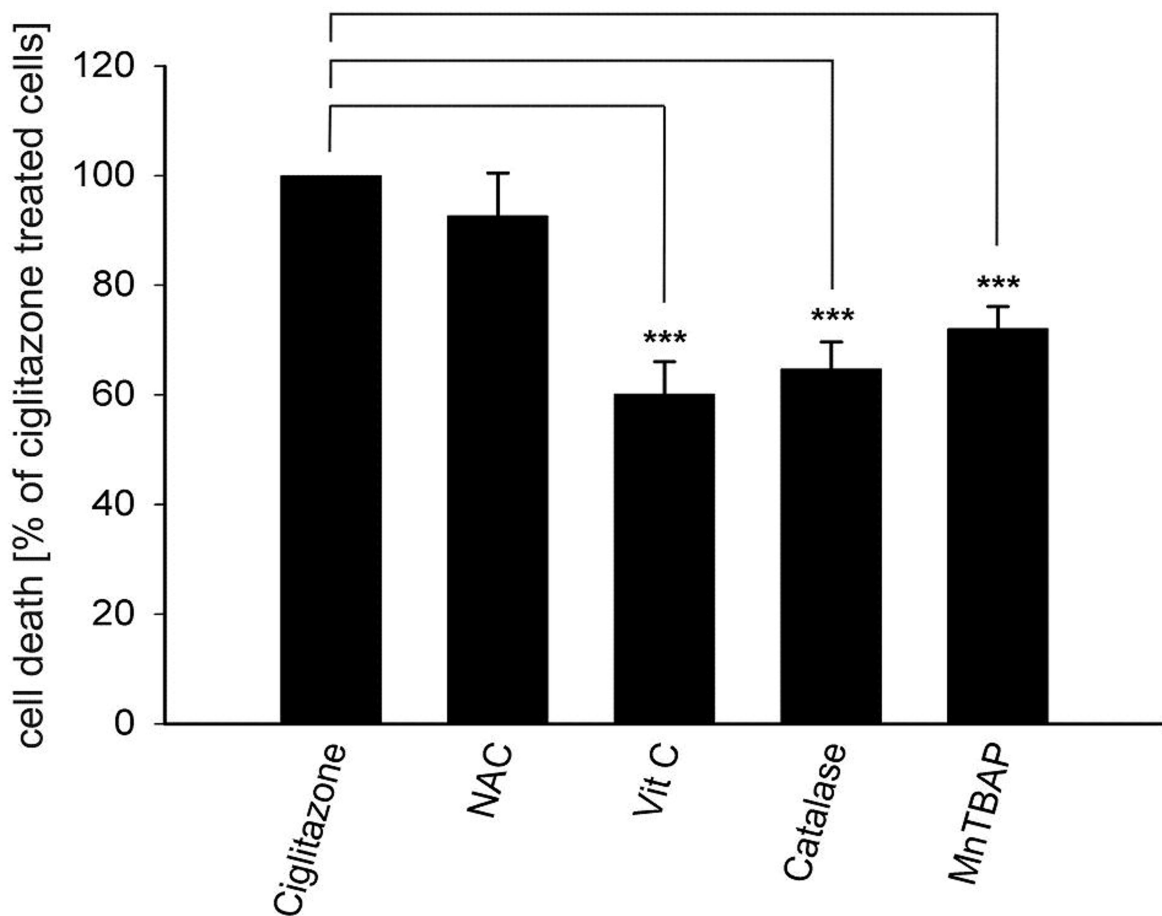


Figure 5



# Figure 6

A



B

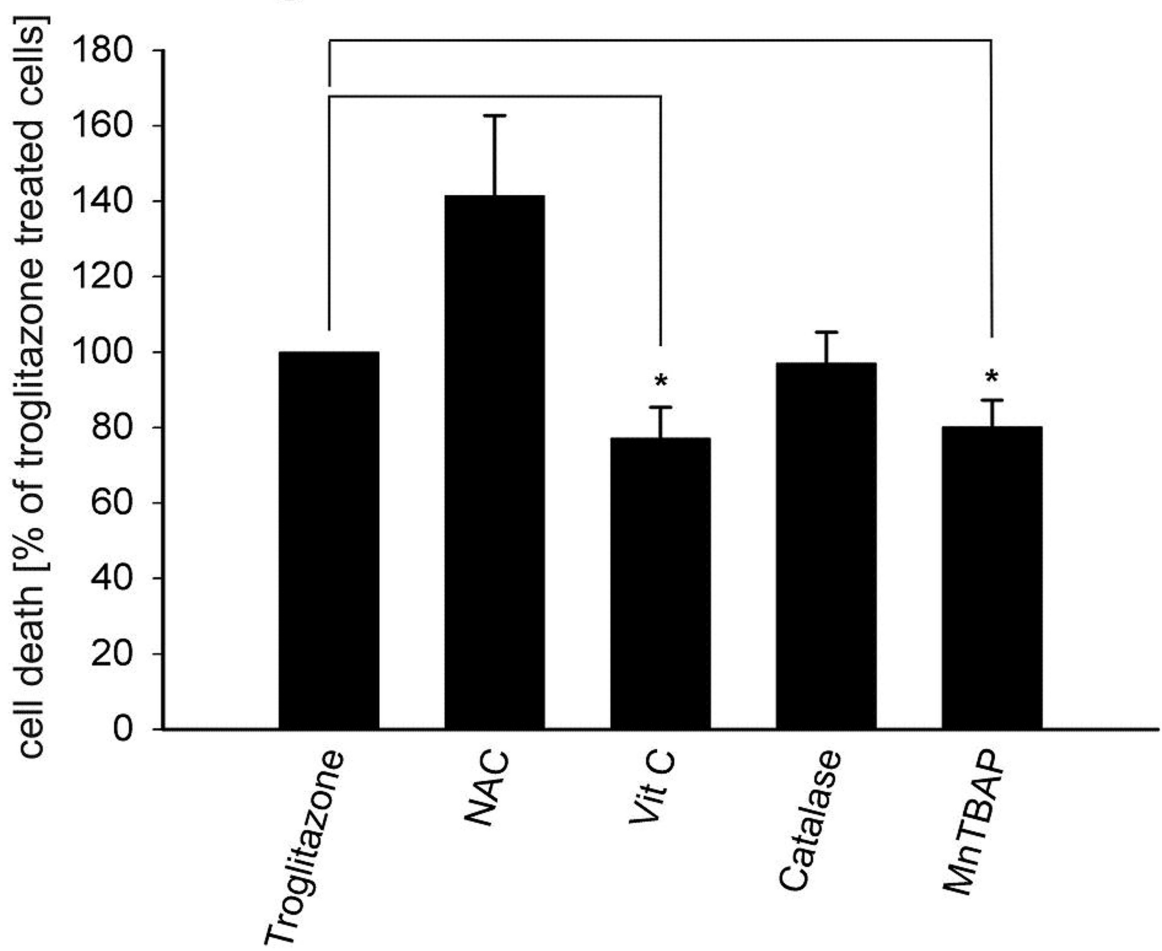


Figure 7

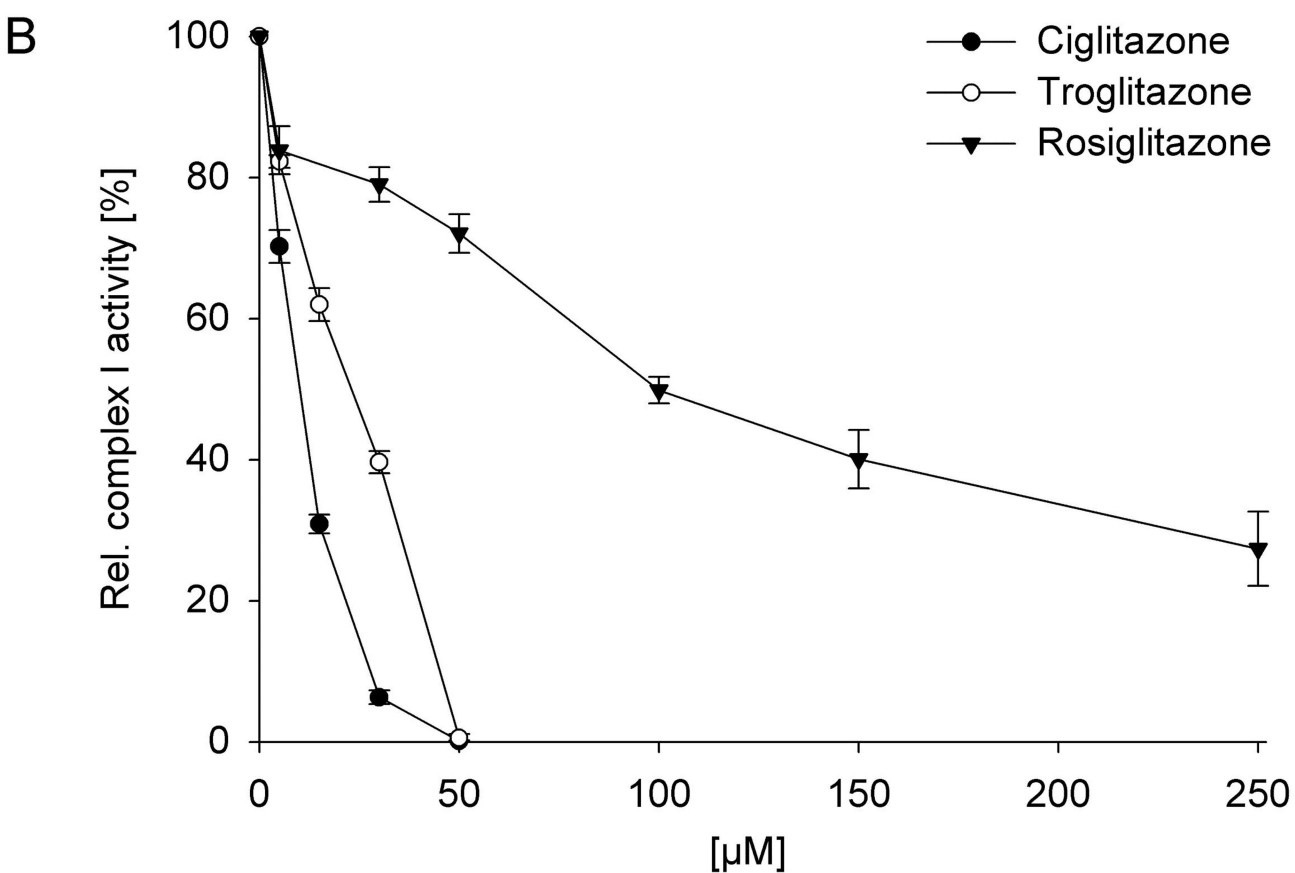
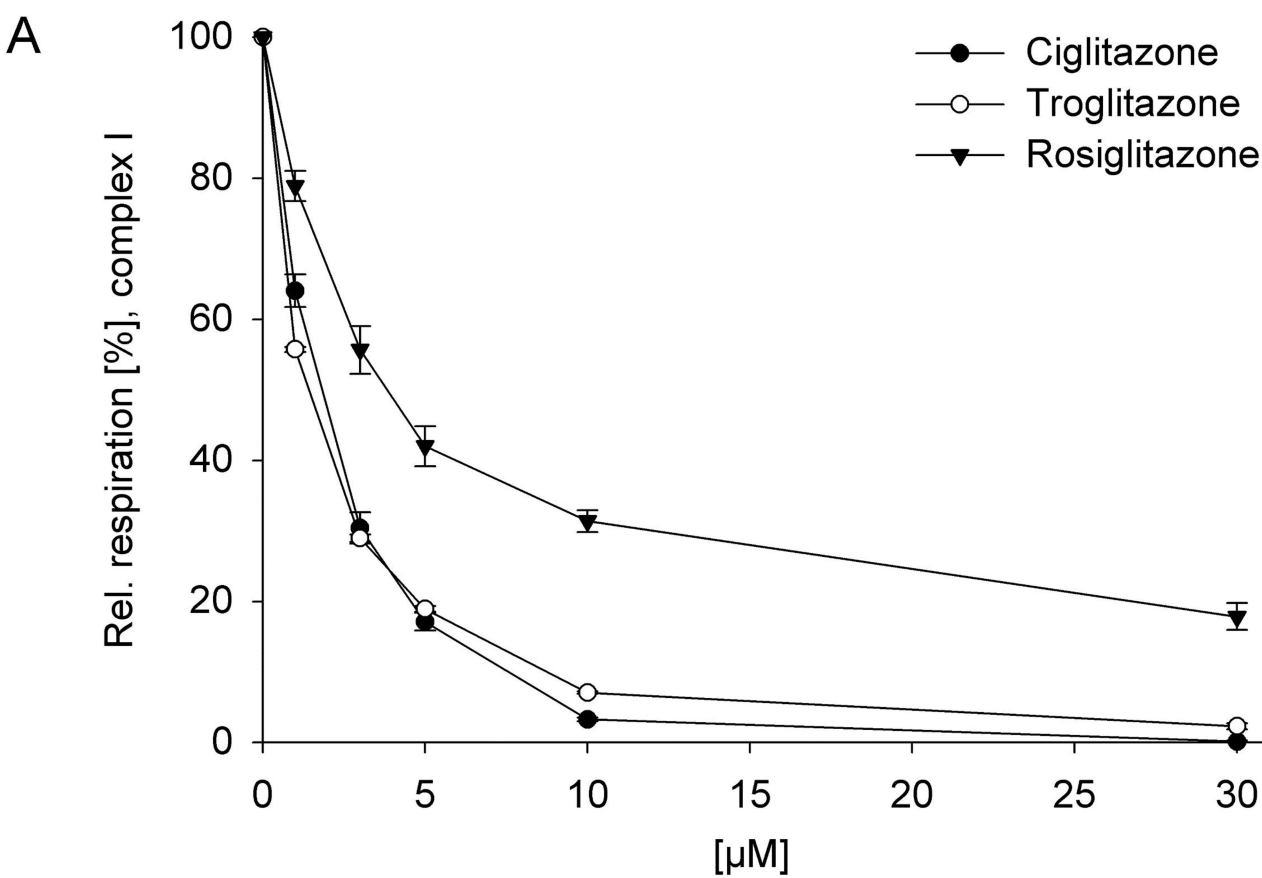
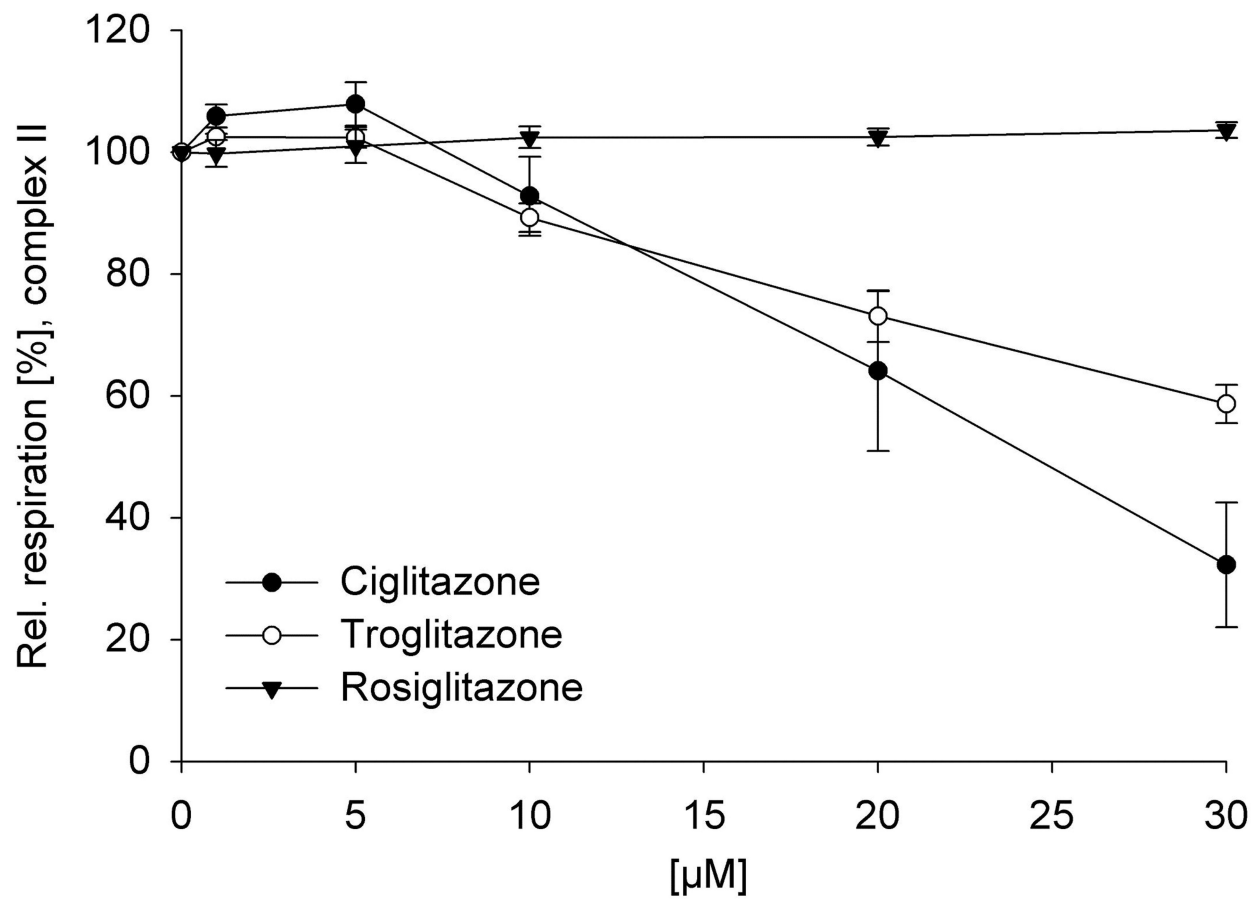
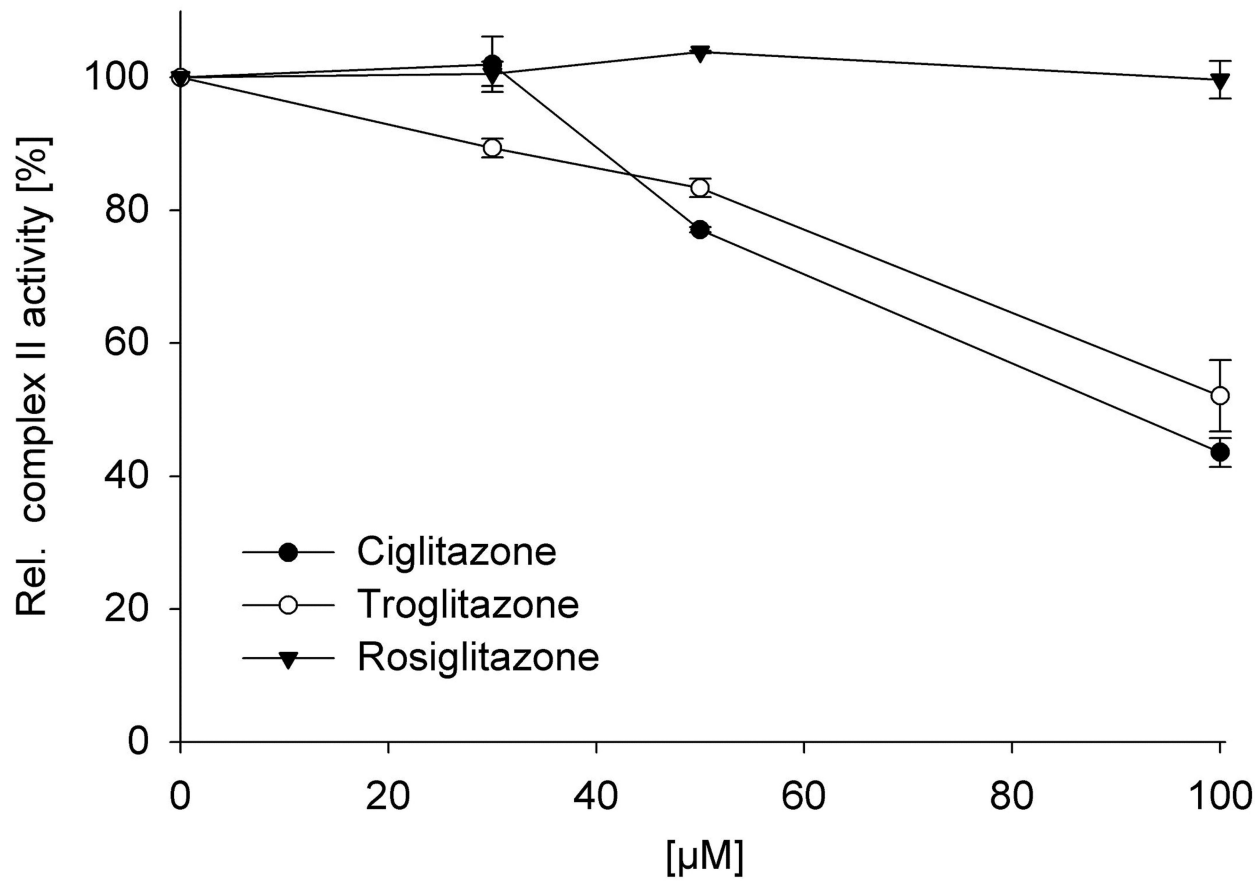


Figure 8

A

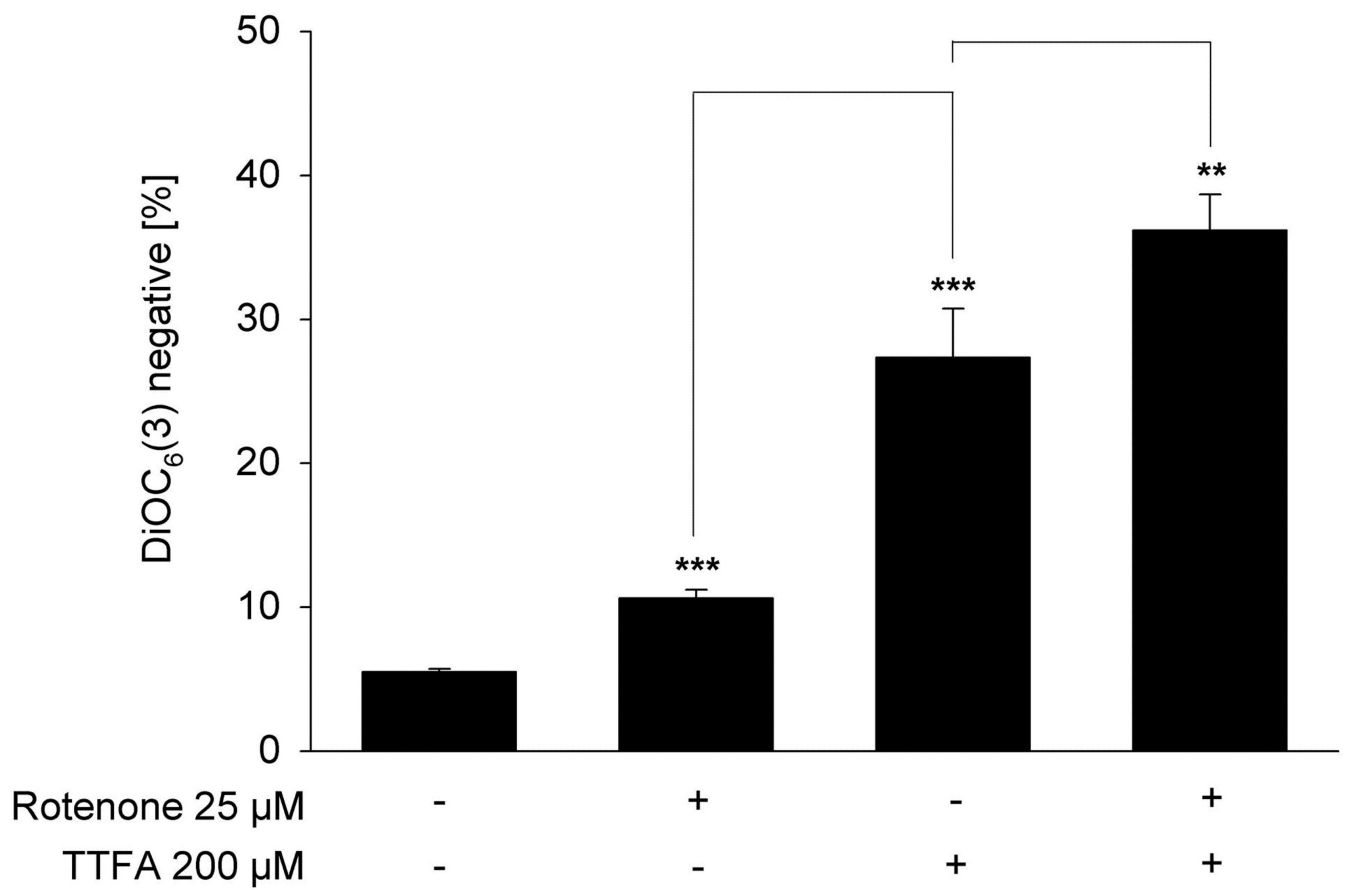


B



# Figure 9

A



B

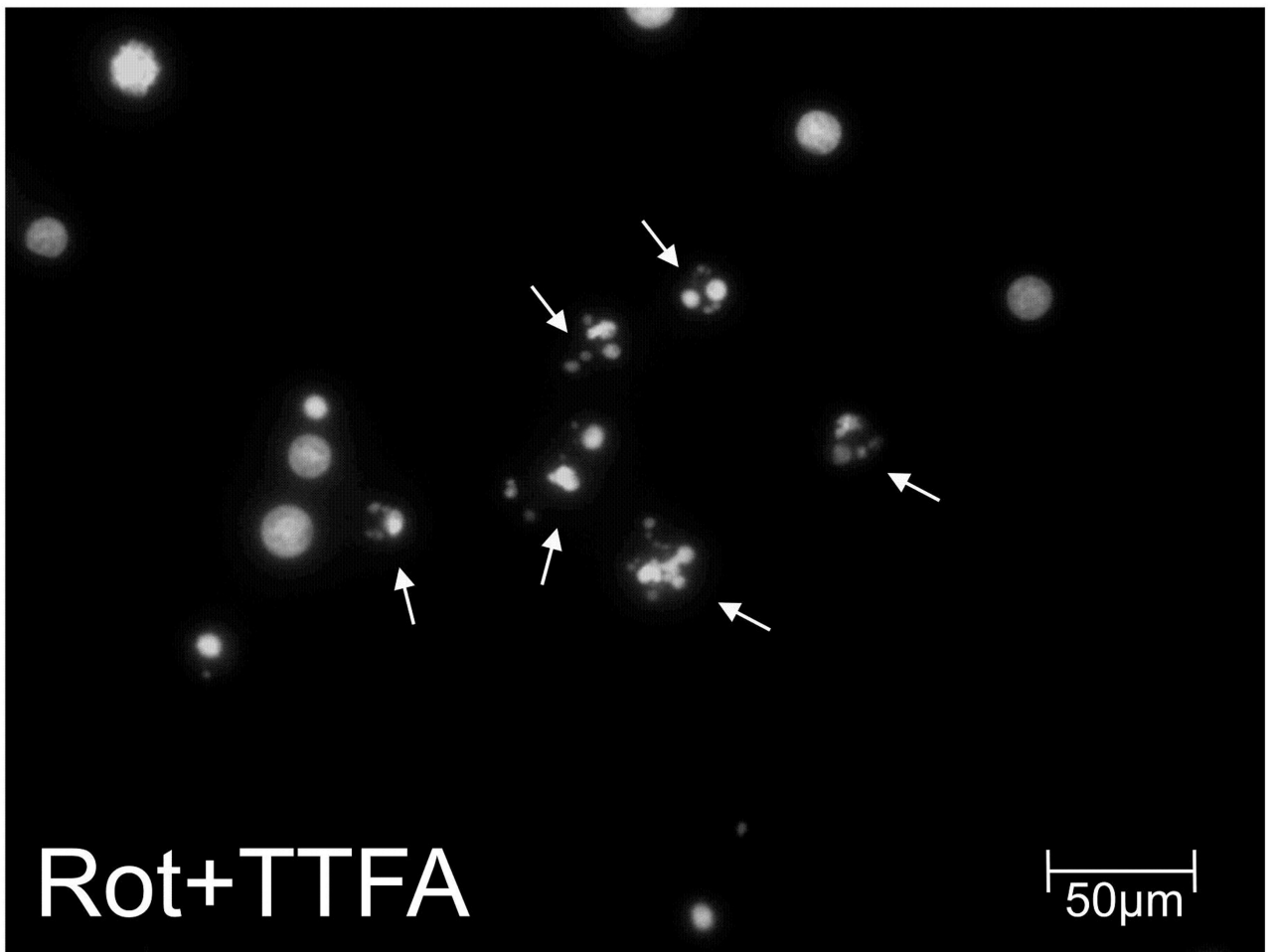


Figure 10

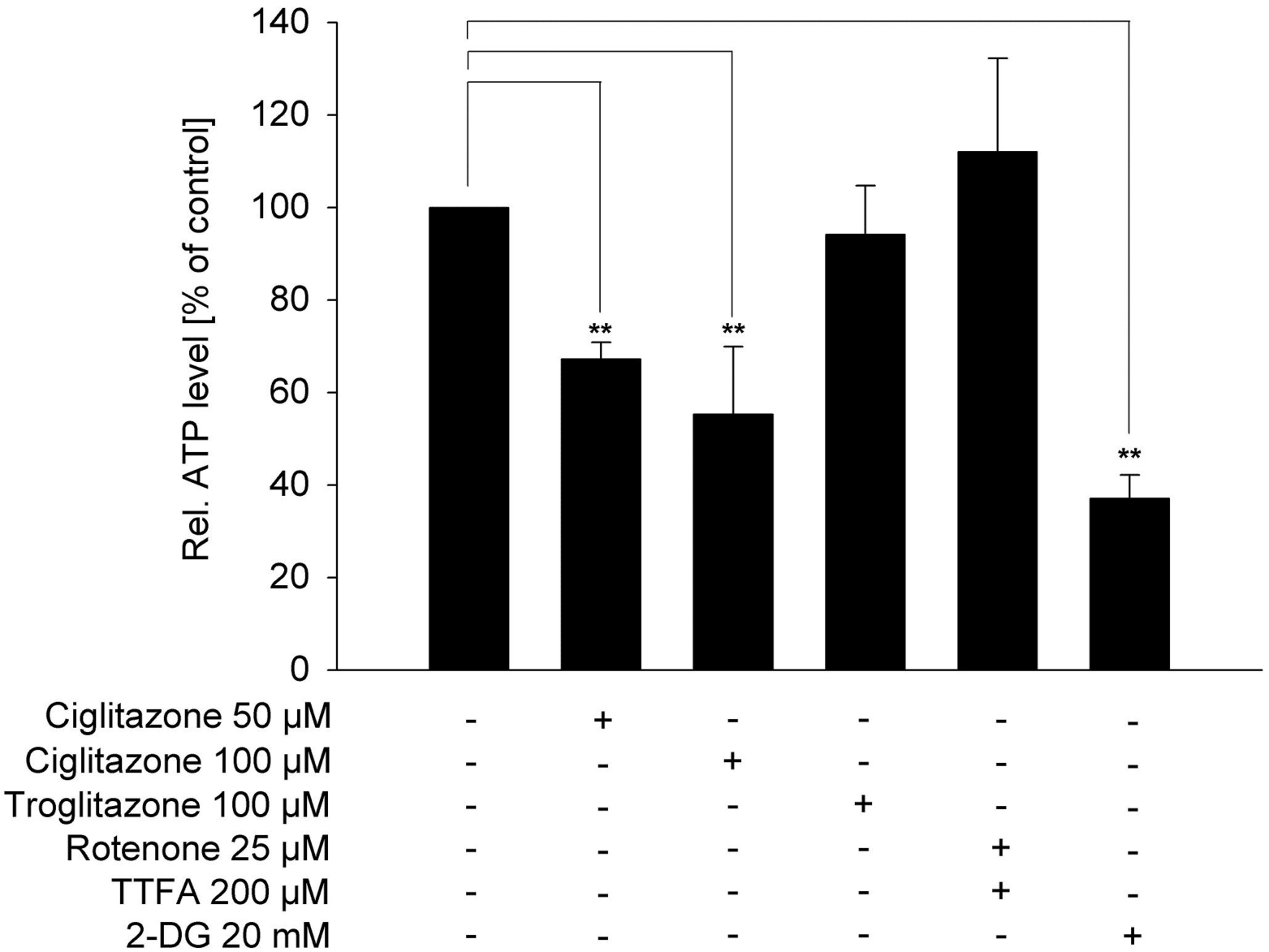


Figure 11

